FUNCTIONAL ROLE OF TROPOMYOSIN ON THIN FILAMENT

ACTIVATION AND CROSS BRIDGE KINETICS IN TRANSGENIC

CARDIAC MUSCLE: A MODEL STUDY

A Thesis

by

GAYATHRI KRISHNAMOORTHY

Submitted to the Office of Graduate Studies of
Texas A&M University
in partial fulfillment of the requirements for the degree of

MASTER OF SCIENCE

December 1999

Major Subject: Biomedical Engineering

FUNCTIONAL ROLE OF TROPOMYOSIN ON THIN FILAMENT

ACTIVATION AND CROSS BRIDGE KINETICS IN TRANSGENIC
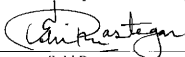
CARDIAC MUSCLE: A MODEL STUDY
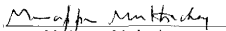
A Thesis

by

GAYATHRI KRISHNAMOORTHY

Submitted to Texas A&M University
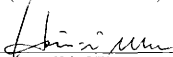in partial fulfillment of the requirements
for the degree of

MASTER OF SCIENCE

Approved as to style and content by:
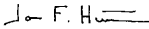
_____
Sohi Rastegar
(Co-Chair of Committee)

_____
Mariappan Muthuchamy
(Co-Chair of Committee)

_____
Hsin-I Wu
(Member)

_____
Jon F. Hunter
(Member)

_____
Way Kuo
(Head of Department)

December 1999

Major Subject: Biomedical Engineering

ABSTRACT

Functional Role of Tropomyosin on Thin Filament Activation and Cross Bridge Kinetics in

Transgenic Cardiac Muscle: A Model Study. (December 1999)

Gayathri Krishnamoorthy, B.E., University of Mumbai, India

Co-Chairs of Advisory Committee: Dr. Sohi Rastegar
Dr. Mariappan Muthuchamy

Regulation of contractile activity in cardiac muscle is a cooperative interaction between thick and thin filament sarcomeric proteins. Tropomyosin (Tm), an essential thin filament protein, interacts with troponin (Tn) and regulates muscle contraction in a Ca^{2+}-dependent manner. Striated muscle-specific α-Tm isoform is the predominant isoform in the adult vertebrate heart, while both α- and β-Tm striated isoforms are present in skeletal muscles. Studies have shown that exchange of myofibrillar proteins can be achieved via a single transgenic manipulation with no change in the stoichiometry of myofibrillar proteins. One of the mouse models with exchange of β-Tm for α-Tm demonstrates that altering the ratio of α- and β-Tm leads to physiological change in myocardial relaxation and increases Ca^{2+} sensitivity of myofilaments. In addition, reduction in maximum force and ATPase activity in this transgenic mouse model suggests no change in the rate-limiting step of cross-bridge detachment. To further understand the mechanisms of how Tm isoform population modulates cardiac muscle dynamics, this study uses a modeling approach. Although existing models address thin filament activation and cross-bridge kinetics, cooperative interactions among myofibrillar proteins have not been explicitly demonstrated. In this study, Tn, Tm and actin are introduced as three different variables to analyze thin filament activation and cross-bridge cycling. The model is initially tested for normal output using data from literature obtained from in vitro and in vivo experiments. Using this model and data obtained from β-Tm transgenic mouse experiments, key parameters that determine functional alteration in the transgenic mouse hearts are identified. Results show that increased calcium sensitivity and decreased maximum force in β-Tm transgenic mouse hearts is due to increased capability of strong cross-bridges in activating the thin filament and decreased rate of attachment of myosin heads to actin.

ACKNOWLEDGEMENTS

TABLE OF CONTENTS

LIST OF FIGURES

LIST OF TABLES

1. INTRODUCTION

1.1. Overview

Cardiac muscle contraction is a result of complex steric, allosteric and cooperative interactions between thick and thin filament sarcomeric proteins, myosin (M), actin (A), tropomyosin (Tm), and the troponin (Tn) complex. This process is driven and regulated by calcium (Ca^{2+}), which is transported into and out of muscle cells via membrane Ca^{2+} channels, causing contraction and relaxation respectively. Ca^{2+} ions then bind to troponin C (TnC) and cause a conformational change that moves Tm from an 'off' state to an 'on' state and exposes actin sites for interaction with myosin heads (cross bridges; CBs) (12,15,23,40). The allosteric model of activation suggests that Ca^{2+} binding to Tn may be insufficient to turn the filament fully 'on', and that the role of Tm is to affect the kinetics of actin-myosin ATPase activity rather than physically block interaction (8,15,17). In this model, Ca^{2+} acts as a cofactor along with myosin CBs in activating thin filament and CB activity, powered by adenosine triphosphate (ATP) (38).

In the myocardium, extent of contraction or twitch is adjusted on a beat-by-beat basis in order to maintain stroke volume and cardiac output in response to bodily demands. Contractile force produced follows the Frank Starling mechanism, whereby maximum force is observed at an optimal sarcomeric length, below and beyond which force decreases. Force production is also modulated by neuro-humoral sympathetic activity (36).

Change in twitch strength is attributed to changes in Ca^{2+} delivery to the myoplasm, Ca^{2+} sensitivity of the regulatory proteins at the molecular level, and kinetics of CB activity in the sarcomere. Cooperative interactions among the contractile and regulatory proteins in the sarcomere also alters twitch strength. Alteration in kinetics and physiological parameters has been observed under conditions of changed Ca^{2+} (46), force (29), myofibrillar protein phosphorylations (39), and single gene mutations in thick and thin filament proteins (25). However, molecular mechanisms governing these changes are not fully understood.

Tropomyosin (Tm), a α-helical dimer lying along the actin thin filament, plays a central role in the regulatory process by modulating CB activity between myosin and actin (23). Striated muscle-specific α-Tm isoform is the predominant α-Tm isoform in adult vertebrate hearts, while both α- and β-Tm isoforms are present in skeletal muscle (33). Experimental studies on transge-

---

This thesis follows the style and format of *The American Journal of Physiology*.

nic (TG) mouse models showed that an isoform exchange of β-Tm in place of α-Tm in cardiac muscle altered dynamics of relaxation (22), increased Ca^{2+} sensitivity of steady-state force and thin filament activation through strong CBs in skinned myofiber preparations (24). In addition, β-Tm containing myofilaments exhibited decrease in maximum force and ATPase activity (47). Hence Tm isoform expression in cardiac muscle plays a significant role in regulating thin filament cooperativity and CB kinetics.

Although it is known that Tm and other myofibrillar proteins play a role in determining CB kinetics, the exact manner in which this regulation is achieved by different proteins is unknown. Numerous models have been formulated that explain different aspects of thin filament activation, CB activity and their regulation. Steric (12) and allosteric (8) models have established the role of Ca^{2+} in thin filament activation. More recent models include cooperativity between thick and thin filament interactions in activating the CB cycle, as a means to better understand the mechanism (3,34). This research proposes a model that includes individual thin filament proteins as determinants of thin filament activation and CB kinetics. A model that incorporates individual thin filament proteins as factors can be used to study other regulatory proteins in their natural and modified forms and their effects on regulation of CB activity. This research describes and applies the model to explain effects of Tm alteration on thin filament activation and CB kinetics in cardiac muscle.

The remainder of this chapter provides a statement of the problem, together with a brief summary of previous work undertaken in the field. This is followed by a detailed description of the model itself and the results obtained from this study. Finally, a thorough discussion of the results, followed by conclusions and future work to be done is presented.

1.2. Physiological Parameters of Cardiac Performance

(Reviewed in Sherwood (36) and Squire (40)). Cardiac muscle contraction is initiated and maintained by distribution of action potentials produced by pacemaker cells in the heart. These potentials originate in the SA node and propagate via the Bundle of His and Purkinje fibers to initiate sequential contraction and relaxation of the atria and the ventricles. The volume of blood circulated in the body depends on the contractile efficiency of the heart, which in turn depends on factors such as stroke volume, rates of contraction and relaxation, and volume of venous return. Stroke volume is defined as the volume of blood ejected by the ventricles during each contraction. As such, stroke volume is dependent upon force exerted by the ventricle and

residual volume in the ventricle after every contraction. Residual volume varies with changes in filling rates, in order to maintain constant stroke volume. Force of ejection varies with initial sarcomeric length (which partly depends on amount of filling during relaxation). With both residual volume and force of ejection indirectly dependent on filling during relaxation, any change in relaxation rate will directly affect stroke volume by change in filling rates, residual volume, and force production and in subsequent cycles of contraction can impair the cardiac cycle.

1.3. Sarcomere - The Functional Unit of Cardiac Muscle

Cardiac muscle consists of individual fibers with diameters varying between 10 and 100 microns (12,36,40). An individual fiber is made up of number of parallel elements called myofibrils, each of which measures about a micron in diameter. Each myofibril consists of a regular arrangement of thick and thin filaments that is repeated throughout the length of the myofibril, giving it a banded appearance (See Fig. 1). The A bands are made up of thick filaments which are about 1.5 microns in length and about 160 angstroms in diameter. The lighter I bands are composed of thin filaments which are about 2 microns in length and 50 to 70 angstroms in diameter. The I band is divided into two by the Z-line. The space between two Z-lines, typically 2-3 microns long, is called the sarcomere, the functional unit of the muscle.

The organization of filaments in the sarcomere is such that about half the length of a thin filament and two-thirds of the length of an adjacent thick filament overlaps. In the region of overlap in a relaxed fiber, the array contains twice the number of thin filaments as thick ones. Thin filaments terminate at the edge of the H zone, a region of low density in the center of the A band. In the center of the H zone lies the 'pseudo H zone', a region of even lower density, whose width is independent of change in muscle length. This light zone surrounds a thin, dark strip known as the M line.

Each thick filament is mainly composed of several hundred myosin (M) molecules. A myosin molecule consists of two identical subunits, each shaped like a golf club. The rod ends of the protein are intertwined around each other, with the two globular heads projecting out at one end. Many such myosin molecules are staggered lengthwise in hexagonal array in the sarcomere with rods oriented toward the center of the sarcomere and globular heads protruding outward at regularly spaced intervals (See Fig. 2). The rods bear the load of contraction during shortening while the heads form CBs (CB) with the thin filament and carry on ATPase activity. The thin

filaments (See Fig. 3) are composed of three main proteins: actin (A), Tm and Tn. Actin molecules, spherical in shape and arranged in two strands, are twisted together in a double helical structure to form the backbone of the thin filament (Fig. 3 shows a single strand only). The regular arrangement of thick and thin filaments in the sarcomere gives rise to an alternating dark and light banded appearance of the myofibril when viewed with a light microscope.

Each actin molecule has a binding site for attachment to myosin head (S1) to form a CB. In the relaxed state, Tm, a threadlike protein that lies end-to-end alongside the groove of the actin spiral, covers CB binding sites. Thus, it blocks thick and thin filament interaction, thereby inhibiting muscle contraction. Tm is stabilized in this blocking position by Tn, a protein complex consisting of three polypeptide units: one that binds to Tm (TnT), one that binds to actin (TnI) and a third that can bind with calcium (TnC). Besides the seven main proteins, there are several minor proteins that contribute to the structural and functional stability of the sarcomere. The whole sarcomere and the myofibrillar space contains a kind of muscle cytoskeleton, comprising intermediate filaments outside the myofibrils and predominantly an 'elastic' protein termed 'connectin' or 'titin' within the myofibril.

At each junction of the A band and the I band, the muscle surface membrane dips into the fiber to form a transverse tubule (T tubule). A network of interconnected tubules, known as sarcoplasmic reticulum (SR), further surrounds each myofibril. The SR has lateral sacs that store Ca^{2+}.

1.4. Contractile Activity

Contraction occurs when myosin in the thick filament binds with actin in the thin filament and changes conformation, pulling the thin filament inward and producing a change in length (36,40). This process is aided and regulated by Ca^{2+}. During an action potential, developed by the SA node and transmitted via the Bundle of His and Purkinje fibers, Ca^{2+} diffuses into the cytosol across the T tubule membrane. This Ca^{2+} is not sufficient to activate the contractile machinery but is adequate to trigger release of Ca^{2+} stores from the SR. Further, during an action potential, Ca^{2+} also diffuses from the extra-cellular fluid, across the surface plasma membrane, into the cytosol. This triggers further release of Ca^{2+} stores from the SR. When released Ca^{2+} binds to TnC, the molecule changes conformation, increasing affinity of TnI to TnC, simultaneously decreasing its affinity to actin. In addition, the conformation change
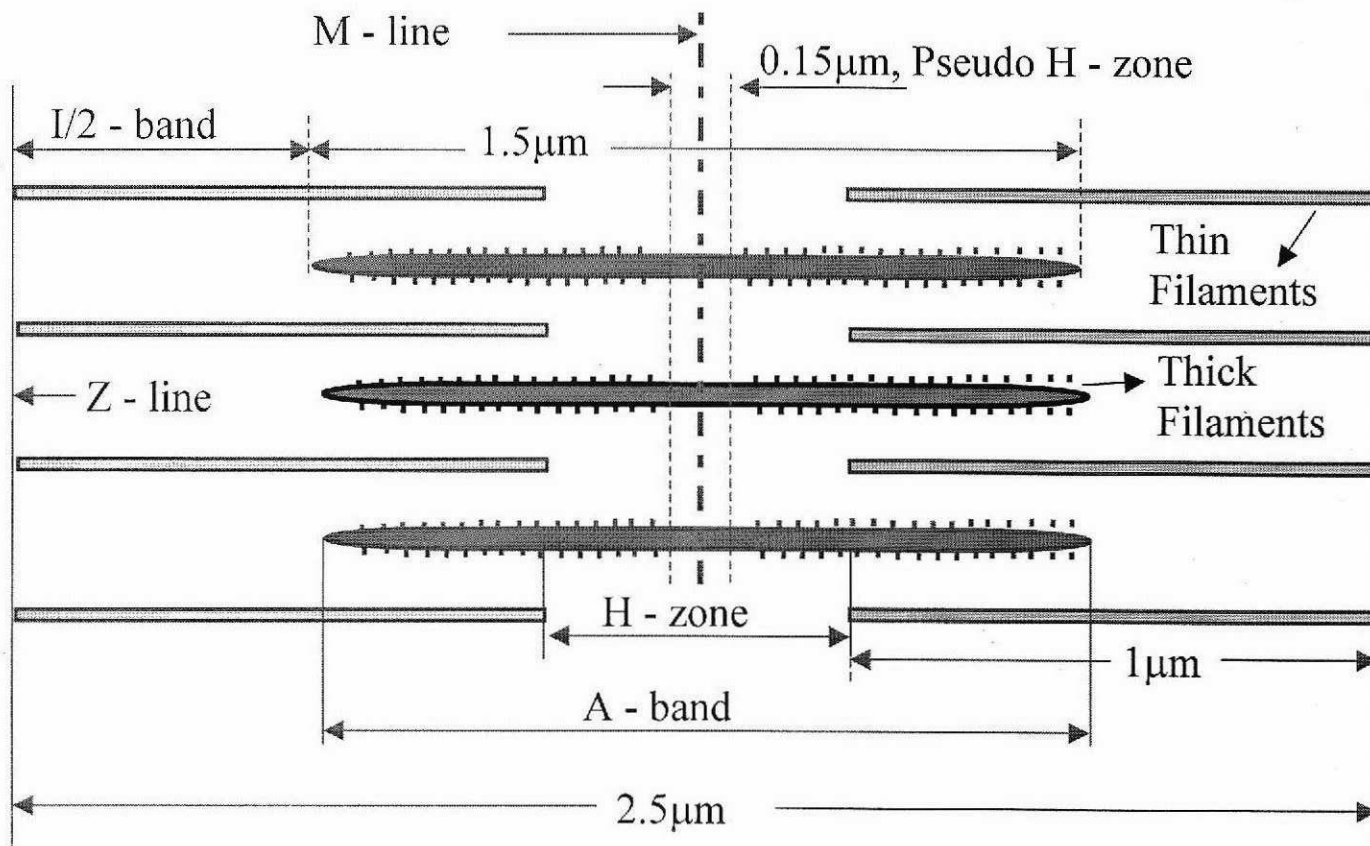
Fig. 1. Organization of a Sarcomere

Myosin Rod

Myosin Head

143 A°
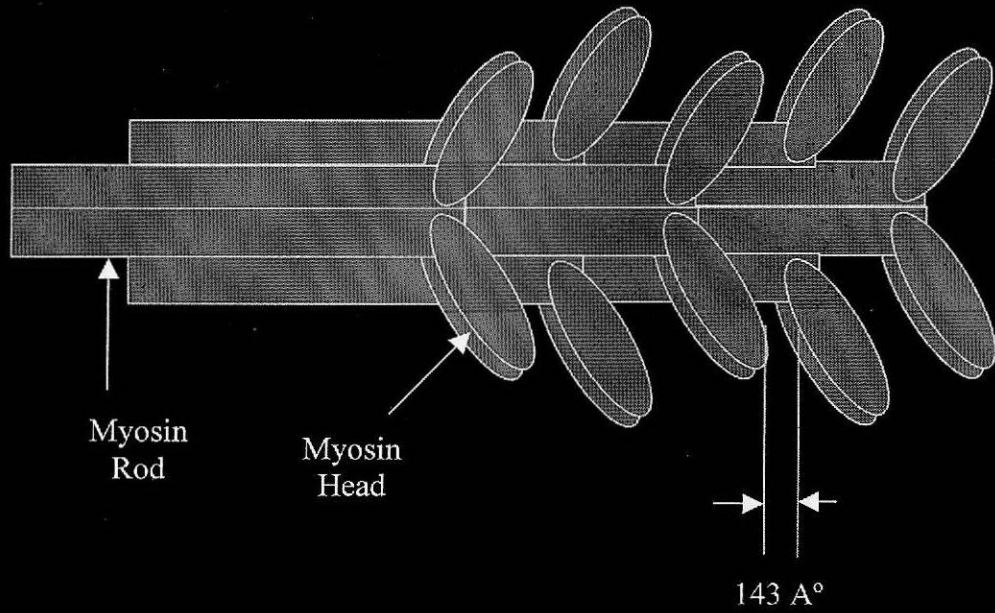
Fig. 2. Organization of Myosin Molecules in Thick Filaments

Actin

Tropomyosin

TroponinC

TroponinI

TroponinT
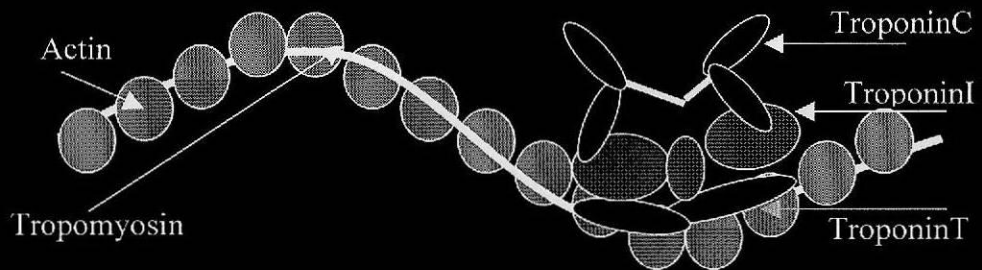
Fig. 3. Organization of Thin Filament Proteins

is transmitted via TnT, rotating Tm such that it slides away from CB binding sites on actin. This facilitates binding of a myosin head (S1) to actin, forming the CB and changing conformation, leading to a 'power stroke' that pulls the thin filament inward. Repeated cycles of this motion cause shortening of sarcomeres along the length of the myofibril resulting in contraction of the fiber as a whole (See Figs. 4A, B). The CB cycle is powered by ATP, which attaches itself to S1, causing it to detach from actin. In the detached state, S1-bound ATP hydrolyses into adenosine diphosphate (ADP), inorganic phosphate (Pi), and chemical energy that is stored in S1. Force production is closely associated with release of hydrolysis products and the stored energy, as soon as S1 binds to actin. This allows the head to change conformation while bound to actin, causing the thin filament to slide inward.

1.5. Familial Hypertrophic Cardiomyopathy

Hypertrophy is an adaptive response of heart muscle to overload or certain 'stress' conditions (28). It involves growth of heart cells without cell division. Hearts exhibiting hypertrophy have thicker ventricular walls and reduced elasticity. Although this increases the mass of the heart and hence potentially its strength, ultimately it leads to decreased cardiac performance. Familial Hypertrophic Cardiomyopathy (FHC) is inherited as an autosomal dominant trait and causes unexplained cardiac hypertrophy. Hearts of FHC patients are characterized by reduced relaxation rates, hypercontractility, and reduced compliance. This leads to a reduction in left ventricular (LV) volume capacity and rapid emptying of a small stroke volume resulting in little or no volume reserve. In some cases, the mitral valve comes into contact with the thickened LV septum, which produces an outflow obstruction. FHC often leads to sudden death usually at the onset of strenuous exercise (25).

The genetic disorder underlying FHC causes structural defects in heart tissue that make it less elastic and unable to withstand high heart rates. Dysfunction arises when mutations affect proteins of the cardiac sarcomere, source of heart muscle contraction. Several distinct single-gene mutations in genes encoding sarcomeric proteins have been identified through extensive study of the genetic mechanisms of FHC. Mutations have been discovered in cardiac (beta)-myosin heavy chain (cβ-MHC), cardiac troponinT (cTnT), cardiac troponinI (cTnI), (alpha)-tropomyosin (α-Tm), ventricular myosin essential light chain (MLC), and cardiac myosin-binding protein C (cMy-BPC) (2,28,39,25). All these mutations affect some aspect of contractile regulation of the myofiber at the molecular level and hence lead to reduction in contractile

efficiency as a whole. A detailed knowledge of interactions between contractile proteins that bring about muscular contraction is essential in order to understand the effects of genetic variations observed in FHC phenotypes.
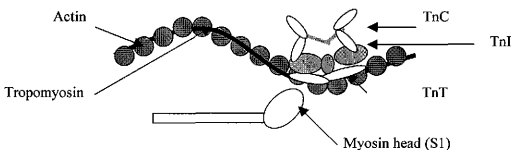
Fig. 4A. Interactions Between Thick and Thin Filament Proteins During Diastole
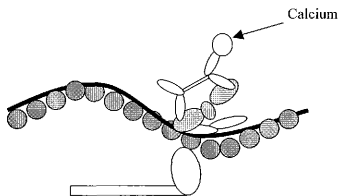
Fig. 4B. Interactions Between Thick and Thin Filament Proteins During Systole

1.6. Thin Filament Regulation

Regulation and activation processes in cardiac muscle are the result of highly complex protein-protein interactions triggered by Ca^{2+} binding to thin filament. Understanding molecular mechanisms of signal transmission between thin filament Ca^{2+} binding and promotion of CBs from relaxed to force-generating states is one of the main research objectives in this field.

1.6.1. Role of Troponin (Tn)

Triggering of actin-myosin interaction involves movement as well as rotation of Tm on the thin filament and a change in actin structure (38). Initial events that trigger state change are binding of Ca^{2+} to cardiac TnC (cTnC) and transmission of this signal to cTnI. As a consequence, cTnI moves from its diastolic 'off' state (tightly bound to actin) to its systolic 'on' state (tightly bound to cTnC). The inhibitory peptide, by virtue of its interaction with actin, is important not only in the signalling cascade of thin filament activation, but also in regulating actin-myosin interaction in an allosteric fashion. The functional significance of cTnI lies in its ability to affect Ca^{2+} sensitivity of thin filament activation when certain sites on the peptide undergo phosphorylation. Decrease in Ca^{2+} sensitivity, decrease in maximum ATPase activity with no change in Ca^{2+} sensitivity, decrease in affinity of S1 for the thin filament are some of the effects observed in experiments when different interacting sites on cTnI are phosphorylated.

Being the longest and the biggest component of cTn, cTnT has the most extensive and versatile interactions with adjacent thin filament proteins. cTnT extends to about one-third the length of Tm and has two regions of high-affinity interaction with actin-Tm. One region anchors the cTn complex to Tm regardless of Ca^{2+} concentration in the surroundings, while the other region forms a complex with cTnC, cTnI and Tm. The first region (TnT1) binds at the overlap of two contiguous Tm molecules and determines the size of the cooperative unit, while the second region (TnT2) is crucial to transmission of the Ca^{2+} binding signal that switches on and activates the thin filament. Phosphorylation of these sites brings about a decrease in the ATPase activity while maintaining Ca^{2+} sensitivity. Interaction sites between cTnT and cTnI are largely undefined.

cTnC binds to Ca^{2+} and starts the triggering process. It is proposed that fast-skeletal TnC (fsTnC) plays a dual role in regulation and release of myofilaments from TnI inhibition and potentiation of myofilament activity by a TnC-TnT interaction. Similar observations for cTnC have yet to be made.

1.6.2. Role of Tropomyosin (Tm)

Tropomyosin (Tm) is central to the control of Ca^{2+}-regulated contraction in striated muscle, which, in concert with the Tn complex, controls actin-myosin ATPase activity. Tm also determines the size of the cooperative unit, i.e., the number of actin sites controlled by a single Tm molecule (23). While an independent Tm controls 5 actin sites, in presence of Tn, the

number of actin sites controlled is 10-12 (8). Electrostatic interactions between Tm and actin determine its position on the actin surface at low ionic strengths, and this is seen in the preferential 'off' state position of the Tm molecule in the thin filament (16). As mentioned previously, Tm also interacts with cTnT at two regions. The region TnT1 binds close to the head-to-tail overlap region of Tm, while the region TnT2 forms a complex with Tm, cTnI and cTnC. In the absence of Ca^{2+}, interaction with TnT2 stabilizes Tm in the 'off' state in the thin filament even at physiologic ionic strengths. Ca^{2+} binding to cTnC does not affect the binding of Tm to TnT1; however, binding in the region of TnT2 is dramatically altered. In the presence of Ca^{2+}, TnT2 no longer binds to Tm (26). The binding of S1 to the thin filament further introduces changes in the electrostatic interactions between Tm and actin, causing a large shift in the Tm position and turning 'on' the thin filament.

1.7. Effects of Over-expression of β-Tm in the Heart: A Transgenic Approach

The significance of the role played by Tm in regulation can be appreciated by the fact that Tm isoform composition is associated with contractile speed of a myofiber (23). This suggests that Tm isoform composition plays a contributing role in influencing physiological function. In cardiac muscle, the predominant Tm isoform is α-Tm. During fetal development, α-Tm represents 80% of total Tm in the heart, while 20% is β-Tm. In the adult heart, β-Tm represents 2% of Tm expression, with α-Tm representing 98%. However, in hypertrophied hearts, there is re-expression of β-Tm (33). Numerous biochemical and structural studies and models of Tm have provided evidence of the steric and cooperative effect exhibited by Tm in regulating actin-myosin interaction during thin filament activation (12,17). However, little is known about functional differences among Tm isoforms. One method of studying structural and physiological effects of alterations in protein expression is through the use of transgenic models. Transgenic (TG) animal technology allows one to create over-expression or ablation of a specific protein in order to assess the functional role of that protein as well as compensatory mechanisms which might be activated in response to the alteration in expression (21).

Using such a TG approach, Muthuchamy et al. developed a mouse model of over-expressed β-Tm in cardiac muscle (21). Hearts of these mice showed preferential formation of αβ-Tm heterodimers as compared to αα-Tm homodimers in non-transgenic (NTG) hearts, while introducing no change in expression of other contractile and regulatory proteins. Expression of β-Tm simultaneously caused a decrease in the production of α-Tm such that total Tm content in

the muscle fiber remained the same as in NTG hearts (22). When analyzed for cardiac performance using the isolated work-performing mouse heart preparation, these hearts displayed normal myocardial contractility parameters. As compared to NTG hearts, however, there was a significant delay in time for half-maximal relaxation as well as a decrease in maximum rate of relaxation in the left ventricle (22).

Further experiments were performed on skinned fibers from these hearts to explicitly test effects of alterations in Tm isoforms on myofilament activation (24). Results from these experiments offered evidence that exchange of Tm isoform altered thin filament activation by affecting Ca^{2+} and strong CB binding. TG-β-Tm fibers exhibited increased Ca^{2+} sensitivity as compared to NTG fibers, i.e., less Ca^{2+} was required to achieve a particular sub-maximal force. Moreover, results also indicated that the isoform switch nullified the effect of TnI phosphorylation. Whereas TnI phosphorylation decreased Ca^{2+} sensitivity in NTG hearts, when TnI in the TG myofilaments were phosphorylated, there was no effect on Ca^{2+} sensitivity, indicating that Tm isoform has a role to play in this regard. Moreover, at low Ca^{2+} concentrations, myofilaments from the TG model developed more force than the NTG fibers, indicating greater number of CBs in the strong bound and rigor states in the TG fibers.

Simultaneous measurement of ATPase activity and contractile force resulted in a linear relationship between force and ATPase activity, indicating that CB turnover was unaffected by Tm isoform switching. However, TG-β-Tm fibers demonstrated significantly less tension and ATPase activity at maximum Ca^{2+} concentration than NTG controls. Hence this model provided evidence that relative Tm isoform population modulated dynamics of contraction and relaxation, but did not alter CB turnover, i.e., did not change the rate of detachment of CBs (47).

1.8. Current Status of the Problem

The TG mouse model established the importance of Tm isoform population in cardiac performance. An exchange in the Tm isoform directly affected CB cycling kinetics at both molecular level and macro level and impacted performance of the mammalian heart. However, the exact mechanism that brings about these effects at the molecular level of the functional unit is as yet unknown. It is proven experimentally and described extensively, via models, that Tm is strategic in the allosteric, cooperative activation of the thin filament and CB cycling and hence is central to functioning of the myofilament. The vast amount of biochemical literature and numerous models explaining CB kinetics notwithstanding, the exact co-operativity that exists

between calcium activation and CB activation of the thin filament is, as of now, an unanswered question. Further, there is no standard model to quantitatively compare different mechanisms that occur in NTG and TG systems.

1.9. Mathematical Models

Experimental results are limited by their representation of a particular system under investigation and may be difficult to generalize. Though the experimental results from TG models give new insights into the contractile activity, exact mechanisms that brings about these effects must be determined through other methods. Biomodeling, or mathematical modeling of physiological systems is one such method that can assist in study and analysis of complex, dynamical systems. Modeling a physiological system usually results in a description in terms of equations, usually differential equations, chosen to describe dynamic aspects of a system. A model is described completely by variables chosen and relationships that exist between those variables and other system parameters and constants. A model in which variables are defined as per system requirements and relationships are written according to the principle of conservation will display similar major characteristics as the real system. Mathematical methods of modeling systems lead to better ability to generalize results and to apply them to solution of dynamic problems such as the contractile activity of muscle.

1.10. Early Models

The earliest model explaining muscle contraction was the sliding filament mechanism proposed by Huxley and Hanson in 1954 (40). This model postulated that contraction or shortening is achieved due to thick and thin filaments sliding past each other, while their respective lengths remained constant.

In 1957, A.F. Huxley established the CB theory to explain the process that caused shortening and force production. Later, in 1969, H.E. Huxley extended this theory with the 'swinging CB' model. In this model, force generation and filament sliding are accomplished by myosin projections (CBs) that cyclically attach to and detach from actin filaments. Force is generated by attached CBs, pulling actin filaments in the direction of muscle shortening. Amount of force produced is a linear function of CB strain and energy of contraction is provided by coupling hydrolysis of an ATP molecule to the cycle of CB attachment and detachment.

Lymn and Taylor further extended this theory, suggesting that in absence of ATP, actin-myosin attachment is permanent, as in rigor mortis. Addition of ATP allows a myosin head to detach from actin, and while detached, ATP hydrolysis products, ADP and Pi, are formed to give M.ADP.Pi, but they are not yet released. In this form, myosin heads can rebind to actin and produce force which is associated with release of ADP and Pi, whereupon the rigor-like state (A*M) is re-formed.

1.11. Regulatory Models

Actin-myosin studies by Ebashi's group in 1968, with and without Tm, showed the first indications of actin filament involvement with regulation of contraction (40). Through these studies and regulatory models proposed by Heselgrove, Huxley and Parry & Squire in 1973, the sequence of processes leading to muscle activation was established. Muscle action potentials travel across plasma membrane and down T-tubules into the interior of the fiber. The net result is a release of Ca^{2+} ions into muscle sarcoplasm from SR stores, changing intracellular Ca^{2+} levels from about 10^{-7} to about 10^{-5} M. Over this concentration range, TnC would reversibly and specifically bind to Ca^{2+} ions. This triggers the sideways movement of Tm across the surface of the actin filaments via the change in position of TnT. Movement of Tm either exposes the actin site to which S1 binds or, alternatively, alters this site so that attachment and completion of the ATPase cycle could occur. This model was called the 'steric blocking model' on account of the two states of Tm that either prevent or allow binding of myosin to actin in the absence and presence of Ca^{2+} respectively.

Contradictions to this model appeared in 1985, when studies of the behavior of purified proteins in solution by El Saleh and Potter showed Ca^{2+}-insensitive binding of myosin to the thin filament. Experiments by Chalovich and Eisenberg in 1982 demonstrated that binding of S1s to thin filaments did not correlate well with the activation of ATPase activity. Also, binding of myosin to actin was found to be a cooperative mechanism, implying that binding of one myosin to the thin filament made it easier for more myosin heads to bind to it. Greene and Eisenberg further found that binding of myosin to pure actin is non-cooperative, but in the presence of Tm-Tn, this process becomes highly cooperative, both in the presence and absence of Ca^{2-}. This led to the proposal that, rather than recruiting CBs in an 'all-or-none' fashion, Ca^{2+} increases the rate of a kinetic step in the CB cycle.

In 1980, Hill et al. formulated a model accommodating these observations by defining two states of the actin.Tn.Tm unit - a 'turned on' and a 'turned off' state, dependent on the occupancy of thin filament with CBs. In this model, the thin filament is predominantly in the 'off' state in both the presence and absence of Ca^{2+}. Support for this notion was provided by the work of Ishii and Lehrer (13), who estimated that, even in the presence of Ca^{2+}, only about 2.5% of Tm were turned 'on'. Ca^{2+} binding to Tn only shifted the equilibrium constant between the two states from approximately 0.02 to 0.2. Results from Williams et al. (45), Al-Khayat et al. (1) and Swartz et al. (41) served to support the idea that Ca^{2+} alone is not sufficient to turn the thin filament fully 'on' and facilitate CB cycling and ATPase activity. Rather, Ca^{2+} acts as an allosteric regulator to the binding of myosin heads to the thin filament.

Increasing evidence in this direction led to formulation of new models such as the one by McKillop and Geeves (17). The new model showed thin filaments in three states - a blocked state that cannot readily bind S1, a closed state that can bind S1 but only weakly, and an open state that can bind S1 with high affinity. In this model, Ca^{2+}-induced Tm shift alone is responsible for transition between blocked and closed states, whereas transition from closed to open states occurs due to strong binding of S1. Thus this model incorporates a steric component (blocked to closed transition) as well as a kinetic component (closed to open transition).

1.12. ATPase Cycle

In 1985, Hibberd's group found that the force-generating step in the CB cycling process, regulated by Ca^{2+}, is closely coupled with release of Pi from the high-energy S1 (40). A recurring question was whether Ca^{2+} regulated the CB cycling process in an 'all-or-none' or 'graded' fashion. The steric hindrance model had Ca^{2+} functioning as a switch, recruiting additional actively cycling CBs, which then exhibited maximal cycling kinetics. Alternatively, Ca^{2+} affected rate constants governing transitions between non-force generating (weak bound) and force-generating (strong bound) CBs, thus modulating distribution of CBs between these states, whereas total number of CBs always remained constant. More specifically, whereas the steric model implied no CBs in the relaxed state, there was evidence that substantial population of CBs bound weakly to the thin filament in relaxed state. It was also shown that ATPase activity could occur without S1 having to detach from the thin filament (27,29). Extensive studies on actin-myosin ATPase activity in solution have identified and characterized many intermediate

steps in the ATPase cycle, leading to a number of complex CB models (30,31,32). However, most of the steps can be incorporated into the simplified scheme in Fig. 5 (31).

In this model, ATP binds to S1 (or myosin; M) of an attached (rigor) CB (step 1), followed rapidly by the dissociation of actin (A) from S1 (step 2), producing the detached M.ATP CB state. After hydrolysis of phosphate (step 3), a low-force weak bound A~M.ADP.Pi state is formed (step 4), which is in rapid equilibrium with the M.ADP.Pi state. During isometric contractions, the CB isomerizes to a strong bound state (step 5) producing strain and resulting in force generation (denoted by *). Thin filament activation processes regulate this transition (17,31). Suggestions were made regarding a Ca^{2+}-regulated transition occurring from weak bound low-force A~M.ADP.Pi state to an intermediate, strong bound, low-force, A.M.ADP.Pi state preceding isomerization to the force-producing A.M*.ADP.Pi state by Regnier et al. (29). The strong bound high-strain state rapidly stabilizes due to release of Pi (step 6) from the CB. It is followed by slower release of ADP from the CB (step 7) at the end of the power-stroke. All the steps in the CB cycle are not completely characterized as yet, as more experiments and newer sophisticated methods give evidences of intermediate steps in addition to the simple scheme already described above (11,14,19,29,30,31,32,37). Presently, the notion is that the relaxed state comprises of both blocked (unattached) and weak bound CBs.

1.13. Cooperativity

The contractile process exhibits cooperativity in activation of the thin filament as well as the CB cycle. Cooperativity is seen in allosteric regulation and activation of the thin filament by Ca^{2-} and myosin heads. According to Geeves and Lehrer (8), the thin filament is turned fully 'on' only when the myosin head is enabled in the strong bound or rigor state and does not turn
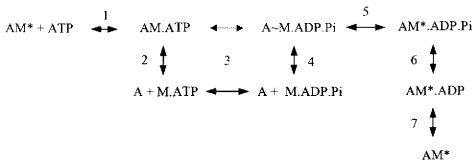

Fig. 5. Basic Cross Bridge (CB) Cycling Scheme

'off' until all actin sites are free of CBs. Cooperativity is also seen in end-to-end interactions of Tm molecules along the length of the actin filament, whereby fully turned on Tm molecules aid the activation of neighboring Tm molecules (34). This in turn feeds into CB cycling, facilitating faster and easier formation of strong CBs. Another kind of cooperativity is the case whereby once a filament is trapped in the 'on' state by strong bound or rigor CBs, subsequent CBs bind to it with relative ease and at a faster rate (34).

Campbell (3) proposed a model to study the effect of such cooperativity on the rate of force production and myofilament activation. This model added to the original two-state CB cycling model (consisting of weak bound and strong bound CBs) a third state of unactivated non-cycling CBs. Transition between non-cycling and cycling CBs is Ca^{2+}-driven at a rate K. Cooperativity was introduced by making K dependent on the population of strong CBs. The model concluded that rate of force redevelopment was enhanced at lower Ca^{2+} levels by formation of strong CBs. However, at higher Ca^{2+} levels, this tended to introduce a counter-effect by slowing rate of force development. Thus cooperativity is most pronounced at basal Ca^{2+} levels, with reduced effect on rate of force redevelopment as Ca^{2+} levels rise.

1.14. Objectives of This Research

All the models described above discuss some aspect of the contractile process such as CB activity (12), thin filament dynamics (8), and Ca^{2+}-regulated cooperativity(3,34). However, there is no standard model that combines all the above as well as include individual thin filament proteins and their interactions and effect on CB kinetics. Such a model would facilitate analysis and prediction of the system output in response to a perturbation in parameters, governed by the differences in properties of protein isoforms. It would also enable one to relate effects of a particular protein change to its specific interactions with other filament proteins. The main objective of this research, therefore, is to develop a model that incorporates both thin filament activation and CB kinetics and their integrated response to Ca^{2+}.

As described previously, changes in thin filament protein expression play a contributing role in filament activation via changes in transmission of the Ca^{2+}-binding signal. The kind of change and the effect on activation and force production due to the change differ from protein to protein. The model proposed in this research pays specific attention to effects of an isoform change in Tm ($\alpha\beta$-Tm as against $\alpha\alpha$-Tm found in nature), introduced in cardiac muscle using a TG approach. Using this TG model, explanations for experimental observations are sought by

examining altered properties between α-Tm and β-Tm in their interactions with other thin filament proteins such as cTnT and actin.

2. METHODOLOGY

2.1. The Model

The model proposed in this research is in close agreement with the model of Geeves and Lehrer (8) and that of Campbell (3). The essential feature of the Geeves model is that in the 'off' state of the thin filament, a myosin head can bind to the it without appreciably affecting the 'on'-'off' equilibrium. However, Tm inhibits isomerization of the CB from a weak bound state to a strong bound state. At high levels of Ca^{2+}, the thin filament dynamically equilibrates between 'off' and 'on' states, with the equilibrium shifted more towards the 'on' state. During the time the filament is transiently in the 'on' state, a bound myosin head in the weak state can rapidly isomerize into the strong bound state, trapping the filament in the 'fully on' state. Campbell incorporated cooperativity in the activation process, by making rate of thin filament switching dependent on population of strong bound CBs, which in turn enhanced CB cycling.

The model proposed here combines features of these two models and additionally incorporates constituent filament proteins in activation of thin filament as well as CB ATPase cycle. Increase in intracellular Ca^{2+} causes TnC to bind to Ca^{2+}. Formation of TnCCa complex causes the Tn molecule to change conformation. This is represented by transition of TnTTm, the Tn subunit bound to Tm, into a conformed state TnTTm'. Rate of this transition is made dependent on population of TnCCa to maintain the stoichiometric ratio inherent in the sarcomeric structure. Thus Ca^{2+} bound to one Tn can cause a conformation change only in one TnTTm subunit. The conformation change on Tn activates thin filament from 'off' state to 'on' state. Two states, Tm_{on1} and Tm_{on2}, define the 'on' states of the thin filament. While transition of thin filament from 'off' to 'on1' is purely Ca^{2+} driven, transition from 'on1' to 'on2' is aided by isomerization of at least one CB from weak bound state to strong bound. Since one thin filament subunit consists of Tn:Tm:actin in a stoichiometric ratio of 1:1:7, it follows that all seven actin sites must be free of bound rigor CBs in order to enable it to revert back to the 'off' state. Ca^{2+} and CB induced activation of thin filament incorporates cooperativity in the model.

The CB cycling section consists of minimum number of steps required for this model. Hence the CB section shows – (a) a detached state, (b) a weak bound state, (c) a strong bound state prior to Pi release, (d) a force producing state after Pi release and prior to ADP release and (e) a rigor state after ADP release. The cooperative nature of the process is evident from the activation-dependent rate of isomerization of a weak bound CB to strong bound state. In absence

of Ca^{2+}, isomerization is prevented and Tm inhibits ATPase activity. However, in presence of Ca^{2+}, isomerization is first aided by a shift in thin filament equilibrium from 'off' state towards 'on1' state. This small increase in isomerization rate, in turn, shifts thin filament equilibrium towards 'on2' state, whereby rate of isomerization is increased to a great extent and the filament is trapped in 'fully on' state. It is evident that such cooperativity would be more prominent at lower Ca^{2+} concentrations, when increase in rate of isomerization would be low. At higher Ca^{2+} levels, rate of ATPase activity and force production would be entirely governed by rates of attachment and detachment of CBs and rate of release of hydrolysis products. Force production is closely associated with release of Pi. Hence the state of the CB prior to ADP release represents a force producing state. A complete diagrammatic representation of the model is shown in Figs 6A and 6B, followed by a detailed description of equations and rate dependencies.

From the Fig. 6A and using standard representation (4), also used by Yamaguchi et al (48), following equations can be written -

$$\frac{d}{dt}\big[TnCCa(t)\big] = k_1\big[Ca(t)\big]\big[TnC(t)\big] - k_2\big[TnCCa(t)\big] \tag{1}$$

$$\frac{d}{dt}\big[TnTTm'(t)\big] = k_3(t)\big[TnTTm(t)\big] - k_4(t)\big[TnTTm'(t)\big] \tag{2}$$

$$\frac{d}{dt}\big[Tm_{on1}(t)\big] = k_5(t)\big[Tm_{off}(t)\big] - k_6(t)\big[Tm_{on1}(t)\big] - k_7(t)\big[Tm_{on1}(t)\big] + k_8(t)\big[Tm_{on2}(t)\big] \tag{3}$$

$$\frac{d}{dt}\big[Tm_{on2}(t)\big] = k_7(t)\big[Tm_{on1}(t)\big] - k_8(t)\big[Tm_{on2}(t)\big] \tag{4}$$

In the above equations, k_1 and k_2 are rate constants governing forward and reverse reactions of Ca^{2+} binding to TnC to form complex TnCCa. Similarly, k_3, k_4 and so on are rates governing forward and reverse reactions in the respective equations. These rates are time dependent since each of them depends on the output of previous steps, which themselves are functions of time.

By species conservation, following equations can be written -

$$TnC + Ca \underset{k_2}{\overset{k_1}{\rightleftharpoons}} TnCCa$$

$$TnTTm \underset{k_4 = f(TnC)}{\overset{k_3 = f(TnCCa)}{\rightleftharpoons}} TnTTm'$$

$$TmA_{off} \underset{k_6 = f(TnTTm)}{\overset{k_5 = f(TnTTm')}{\rightleftharpoons}} Tm_{on1} \underset{k_8 = f(A^*M/7)}{\overset{k_7 = f(A.M.ADP.Pi, TnTTm')}{\rightleftharpoons}} Tm_{on2}$$

Tm$_{on1}$
+
6A
+
A-M.ADP.Pi
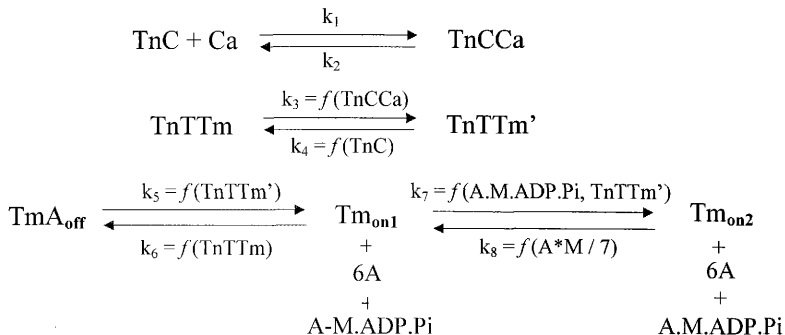
Tm$_{on2}$
+
6A
+
A.M.ADP.Pi

Fig. 6A. Proposed Scheme for Thin Filament Activation

$$A + M.ADP.Pi \xrightleftharpoons[k_{10}]{k_9} A\text{-}M.ADP.Pi \xrightleftharpoons[k_{12} = f(Tm_{off})]{k_{11} = f(Tm_{on1} + Tm_{on2})} A.M.ADP.Pi$$

k_{17} k_{15} k_{13} k_{14}

$$A^*M \xrightleftharpoons[k_{16}]{k_{15}} A.M.ADP$$

A*M
+
ADP

A.M.ADP
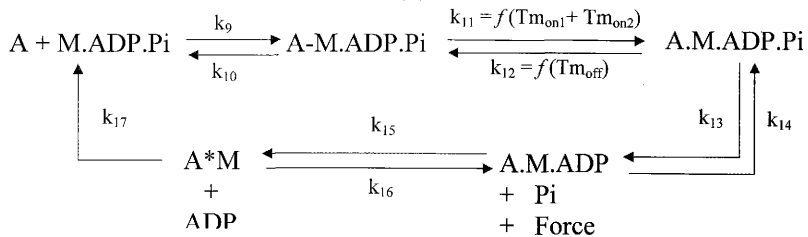+ Pi
+ Force

Fig. 6B. Proposed Scheme for Cross Bridge Cycling

$$[Ca(t)] = [Ca(0)] - [TnCCa(t)] \tag{5}$$

$$[TnC(t)] = [TnC(0)] - [TnCCa(t)] \tag{6}$$

$$[TnTTm(t)] = [TnTTm(0)] - [TnTTm'(t)] \tag{7}$$

$$[Tm_{off}(t)] = [Tm_{off}(0)] - [Tm_{on1}(t)] - [Tm_{on2}(t)] \tag{8}$$

Rates k_3 and k_4 are taken as functions of population of TnCCa in order to make them Ca^{2+}-dependent. Two kinds of relationships are proposed for the rates. The first one is a linear dependence of k_3 and k_4 on the population of TnCCa and TnC as given below -

$$k_3(t) = a_3\big(TnCCa(t)\big) \tag{9}$$

$$k_4(t) = a_4\big(TnC(t)\big) \tag{10}$$

The second one is a saturatable relationship that explicitly includes the stoichiometric ratio of 1:1 for Tn:Tm in the myofilament structure.

$$k_3(t) = a_3\big(TnCCa(t) - TnTTm'(t)\big) \tag{11}$$

$$k_4(t) = a_4\big(TnC(t) - TnTTm(t)\big) \tag{12}$$

The stoichiometric relations ensure that when population of TnTTm' (the conformed complex of TnT and Tm) equals population of TnCCa, the reaction stops by bringing k_3 to zero. Similar reasoning can be given for k_4. Preliminary results showed that the stoichiometric relations are the ones to be used for the model. Hence remaining rate equations will follow the stoichiometric 1:1 relation and the following relations are defined -

$$k_5(t) = a_5\big(TnTTm'(t) - Tm_{on1}(t) - Tm_{on2}(t)\big) \tag{13}$$

$$k_6(t) = a_6 \left(TnTTm(t) - Tm_{off}(t) \right) \tag{14}$$

Since conditions require that transition from state 'on1' to state 'on2' takes place only in presence of at least one strong CB and reverse transition takes place only when all seven rigor CBs are detached, following relations can be written for k_7 and k_8 -

$$k_7(t) = a_7 \left(A.M.ADP.Pi(t) \right) \left(TnTTm'(t) - Tm_{on1}(t) - Tm_{on2}(t) \right) \tag{15}$$

$$k_8(t) = a_8 \left((A*M(t))/7 \right) \tag{16}$$

Inclusion of the 1:1 condition in the relation of k_7 is to ensure that total number of Tm units that are turned 'on' is equal to number of Tn bound to Ca^{2+}. Substituting the rate relations in the original differential equations 1 to 4, we get the final form of the equations for thin filament activation as -

$$\frac{d}{dt} \left[TnCCa(t) \right] = k_1 \left[Ca(0) - TnCCa(t) \right] \left[TnC(0) - TnCCa(t) \right] - k_2 \left[TnCCa(t) \right] \tag{17}$$

$$\frac{d}{dt} \left[TnTTm'(t) \right] = a_3 \left(TnCCa(t) - TnTTm'(t) \right) \left[TnTTm(0) - TnTTm'(t) \right]$$
$$- a_4 \left(TnC(t) - TnTTm(t) \right) \left[TnTTm'(t) \right] \tag{18}$$

$$\frac{d}{dt} \left[Tm_{on1}(t) \right] = a_5 \left(TnTTm'(t) - Tm_{on1}(t) - Tm_{on2}(t) \right) \left[Tm_{off}(0) - Tm_{on1}(t) - Tm_{on2}(t) \right]$$
$$- a_6 \left(TnTTm(0) - TnTTm'(t) - Tm_{off}(0) + Tm_{on1}(t) + Tm_{on2}(t) \right) \left[Tm_{on1}(t) \right]$$
$$- a_7 \left(A.M.ADP.Pi(t) \right) \left(TnTTm'(t) - Tm_{on1}(t) - Tm_{on2}(t) \right) \left[Tm_{on1}(t) \right]$$
$$- a_8 \left(A*M(t)/7 \right) \left[Tm_{on2}(t) \right] \tag{19}$$

$$\frac{d}{dt}\big[Tm_{on2}(t)\big] = a_7 \big(A.M.ADP.Pi(t)\big)\big(TnTTM'(t) - Tm_{on1}(t) - Tm_{on2}(t)\big)\big[Tm_{on1}(t)\big]$$

$$- a_8 \big(A * M(t)/7\big)\big[Tm_{on2}(t)\big] \qquad (20)$$

Equations for the CB cycling part and respective rate relationships can be written in a similar manner. Rates for this part of the model are all constants, taken from literature, except for k_{11} and k_{12}, which are dependent on thin filament activation. This is in keeping with the necessary condition that a weak bound CB can quickly isomerize into strong bound state only when the thin filament is in either of the 'on' states (i.e. 'on1' or 'on2'). Conversely, the thin filament can go from 'on1' to 'on2' only in presence of a rigor CB. This accounts for allosteric cooperativity exhibited by Ca^{2+} and myosin heads in activating the thin filament. In absence of Ca^{2+}, when the thin filament is in neither of the 'on' states, rate of isomerization is greatly reduced, inhibiting ATPase activity. With the above explanation and using Fig. 6B, we can write differential equations for various states in the CB cycle. In the following equations, A represents actin, M.ADP.Pi represents myosin head with the hydrolysis products of ATP, but not yet released, A-M.ADP.Pi is weak bound CB, A.M.ADP.Pi is strong bound CB that has not produced any force yet, A.M.ADP is CB that has released Pi and contributes to active force production and A*M represents CB that has released both ADP and Pi and is bound to actin with high affinity. This is the rigor state of the CB.

$$\frac{d}{dt}\big[A-M.ADP.Pi(t)\big] = k_9\big[M.ADP.Pi(t)\big]\big[A(t)\big] - k_{10}\big[A-M.ADP.Pi(t)\big]$$

$$- k_{11}(t)\big[A-M.ADP.Pi(t)\big] - k_{12}(t)\big[A.M.ADP.Pi(t)\big] \qquad (21)$$

$$\frac{d}{dt}\big[A.M.ADP.Pi(t)\big] = k_{11}(t)\big[A-M.ADP.Pi(t)\big] - k_{12}(t)\big[A.M.ADP.Pi(t)\big]$$

$$- k_{13}\big[A.M.ADP.Pi(t)\big] + k_{14}\big[A.M.ADP(t)\big]\big[Pi(t)\big] \qquad (22)$$

$$\frac{d}{dt}\big[A.M.ADP(t)\big] = k_{13}\big[A.M.ADP.Pi(t)\big] - k_{14}\big[A.M.ADP(t)\big]\big[Pi(t)\big]$$

$$- k_{15}\big[A.M.ADP(t)\big] + k_{16}\big[A * M(t)\big] \qquad (23)$$

$$\frac{d}{dt}[A*M(t)] = k_{15}[A.M.ADP(t)] - k_{16}[A*M(t)] - k_{17}[A*M(t)] \tag{24}$$

Since k_{11} and k_{12} are rates of isomerization of weak bound CB to a strong bound CB, they are dependent on population of Tm_{on1} and Tm_{on2}. Hence we can write relations for k_{11} and k_{12} as -

$$k_{11}(t) = a_{11}\left(Tm_{on1}(t) + Tm_{on2}(t)\right) \tag{25}$$

$$k_{12}(t) = a_{12}\left(Tm_{off}(0) - Tm_{on1}(t) - Tm_{on2}(t)\right) \tag{26}$$

By species conservation, we can write,

$$[A(t)] = [A(0) - (A - M.ADP.Pi(t)) - (A.M.ADP.Pi(t)) - (A.M.ADP(t)) - (A*M(t))] \tag{27}$$

Similar equation can be written for M.ADP.Pi. Equations 1-27 describe the dynamics of the proposed model. Since equations for thin filament activation contain higher powers of dependent variables on the right hand side, the equations are non-linear and do not lend themselves to an analytical solution. Hence, numerical integration is used for solving them. Moreover, the equations have to be solved simultaneously due to the cooperative nature of the process.

2.2. Procedure and Methods

Simulations were run in Matlab with ordinary differential equation (ODE) solvers using Runge-Kutta 4th order. Depending on the stiffness of the problem, the solver dynamically set the time step. Tolerance values were set to the default, i.e., relative tolerance = 1e-3, absolute tolerance = 1e-6. Time span for the runs was set at 48 ms, since this is the observed time for tension development during experiment (7). The model was run for various Ca^{2+} levels ranging from pCa = 7.0 to pCa = 4.5 (pCa = -$\log_{10}[Ca^{2+}]$). Rate constants for the model were chosen from literature and are listed in table 1.

Values for k_1 and k_2 taken from Rosenfeld and Taylor's work (35) are those obtained for fsTnC binding to Ca^{2+}. cTnC and fsTnC differ in the number of regulatory Ca^{2+} binding sites.

Table 1. *Control Parameter Values Used for the Rates in the Model*

Rate	Value Chosen	Source / Reference
k_1	$2e7\ M^{-1}s^{-1}$	Rosenfeld and Taylor, JBC, 1985 (35)
k_2	$150\ s^{-1}$	Rosenfeld and Taylor, JBC, 1985 (35)
a_3	$700\ s^{-1}$	Miki and Iio, JBC, 1993 (18)
a_4	$48\ s^{-1}$	Miki and Iio, JBC, 1993 (18)
a_5	$12.2\ s^{-1}$	Ishii and Lehrer, Biochemistry, 1990 (13)
		Williams et al., Biochemistry, 1988 (45)
		Trybus and Taylor, Proc. Natl. Acad. Sci. USA, 1980 (42)
a_6	$487.8\ s^{-1}$	Same as above
a_7	$1990.05\ s^{-1}$	Coates et al., Biochemical Journal, 1985 (5)
a_8	$9.95\ s^{-1}$	Geeves and Lehrer, Biophysical Journal, 1994 (8)
k_9	$1.5e6\ M^{-1}s^{-1}$	Geeves and Lehrer, Biophysical Journal, 1994 (8)
k_{10}	$25\ s^{-1}$	Geeves and Lehrer, Biophysical Journal, 1994 (8)
a_{11}	$90\ s^{-1}$	Regnier and Homsher, Biophysical Journal, 1998 (29)
a_{12}	$85\ s^{-1}$	Regnier and Homsher, Biophysical Journal, 1998 (29)
k_{13}	$389\ s^{-1}$	Millar and Homsher, JBC, 1990 (18)
k_{14}	$5.6e4\ M^{-1}s^{-1}$	Millar and Homsher, JBC, 1990 (18)
k_{15}	$45\ s^{-1}$	
k_{16}	$9\ s^{-1}$	
k_{17}	$525\ s^{-1}$	Geeves and Lehrer, Biophysical Journal, 1994 (8)

While fsTnC has two of them, in cTnC, one of them is rendered incapable of binding Ca^{2+} due to substitution of an amino acid. However, rates of Ca^{2+} binding to and dissociating from the single site in cTnC and the first regulatory site in fsTnC can be taken as identical.

Hence the second order rate of association of Ca^{2+} binding to TnC is taken as $2e7$ $M^{-1}s^{-1}$ and the first order rate of dissociation is taken as 150 s^{-1}.

Miki and Iio (18) studied the kinetics of structural changes in reconstituted skeletal muscle thin filament by monitoring time course of fluorescence energy transfer between probes attached to TnI and actin. Energy transfer intensity corresponded to rate of conformational change occurring in Tn as a result of Ca^{2+} binding and dissociation. They found that time rate of fluorescence intensity change in low to high Ca^{2+} conditions was 530 ± 170 s^{-1} while that in high to low Ca^{2+} conditions was 43 ± 5 s^{-1}. These values are taken as the values for a_3 and a_4.

Ishii and Lehrer (13) have shown that even in presence of Ca^{2+} only about 2.8% of thin filaments are in the 'on' state. Williams et al (45) have shown that, in absence of any bound myosin head (S1), the thin filament is predominantly in the 'off' state with rate constant of transition between 'off' and 'on' states being approximately 0.2. Trybus and Taylor (42) have further shown through their results that rate of the state change is of the order of 500 s^{-1}. Values for rates a_5 and a_6 are thus calculated from these values as 12.2 s^{-1} and 487.8 s^{-1} respectively.

Values for these and other rates are taken from the sources listed in Table 1. With most of the rates known, rate values k_{15} and k_{16} were estimated by trial and error method. The best values that gave required output for the model were $k_{15} = 45$ s^{-1} and $k_{16} = 9$ s^{-1}.

2.3. The Transgenic Model

Key parameters to be modified for the transgenic (TG) model were identified using the differences in properties between α-Tm and β-Tm.

1. In 1982, Pearlstone and Smillie (26) found that β-Tm bound more weakly to TnT than α-Tm.

2. In 1995, Muthuchamy et al. (22) found that Tm isoform change resulted in FHC phenotypes of decreased maximum rate of relaxation and delay in time for half-maximal relaxation.

3. In 1997, Golitsina et al. (9) studied effects of Tm-FHC mutants and found that Tm-FHC mutants had 2-3 fold decreased affinity to actin, regardless of ionic conditions and presence of Tn with or without Ca^{2+}.

These property changes are thought to impart increased flexibility to the Tm molecule on the actin filament, leading to early switching 'on' of the thin filament as a whole. It is hypothesised that this increase in flexibility could be the reason for increase in Ca^{2+} sensitivity. Hence in the TG model, rate of thin filament switching (controlled by k_5 and k_6) from 'off' to 'on' is identified

as the first key parameter responsible for increase in Ca^{2+} sensitivity. The effect of an increase in a_5 and a decrease in a_6, resulting in an increase in rate of thin filament switching, is studied.

4. Rate of isomerization of CB from weak bound state to strong bound state is dependent on thin filament activation processes (17).

5. From experiments on skinned fibers from the β-Tm model, Palmiter et al. (24) found that at low Mg-ATP, force increased as strong bound rigor CBs activated the thin filament, i.e., the TG model showed increased Ca^{2+} sensitivity of ATPase activity. This observation further supports the hypothesis of an increase in rate of isomerization at low Ca^{2+} levels.

From these observations, the second key parameter identified as a factor leading to increased Ca^{2+} sensitivity in the TG model is rate of isomerization of weak bound CBs to strong bound state. The effect of increase in a_{11} and a decrease in a_{12}, resulting in an increase in rate of isomerization is studied.

6. Wolska et al. (47) found that though Ca^{2+} sensitivity of force and ATPase acitivity was increased, maximum force at high Ca^{2+} levels was reduced in the TG model. This meant that population of CBs in bound but non-force producing state and in unbound state is more as compared to that in force producing states. Moreover, decrease in maximum ATPase acitivity translates to decrease in population of strong bound CBs prior to Pi release. The reason for this could be a decrease in CB turnover, i.e., increase in population of rigor CBs, caused by decrease in rate of detachment of rigor CBs from the thin filament. However, ratio of ATPase activity to force or the "tension cost" was found to be same in both NTG and TG models. Since ratio of ATPase activity to force gives an estimate of rate of detachment, an unchanged ratio meant no decrease in rate of detachment.

7. A reason for a decrease in maximum force could be a decrease in rate of attachment of myosin head to the actin filament (20). This would be expected to decrease the cumulative population of CBs in the strong bound rigor state, leading to decrease in force production.

8. A third reason for decrease in maximum force could be an increase in the population of rigor CBs due to an increase in its rate of formation, without any change in its rate of detachment.

Hence, in order to identify the mechanism for a decrease in maximum force, two options are studied - 1) an increase in the rate of rigor CB formation and 2) a decrease in the rate of CB attachment.

Various combinations of the above parameters are studied for the TG model and the results are presented next. The combination of parameter changes that produced the best fit to experimental data is then thoroughly discussed to evaluate its implications on the myofilament activation and contraction processes.

3. RESULTS

3.1. Results for the Non Transgenic (NTG) Model

Figs. 7A to 7J show results for the NTG (also called wild type (WT), control) model described earlier, obtained with control parameter values specified in the previous chapter. Fig. 7A shows a representative set of time curves for population of TnCCa. For low Ca^{2+} levels (pCa = 7.0), rate of binding to Ca^{2+} is very low and hence the population does not rise above 2% of the maximum. As Ca^{2+} concentration increases, rate of formation as well as steady state population of bound TnC increases until at pCa = 4.5, population reaches its maximum value of approximately 86. Fig. 7B shows a similar set of time curves for increase in population of TnTTm'. Rate of conformation change of TnTTm is controlled by increase in TnCCa, since all the curves closely follow those shown in Fig. 7A.
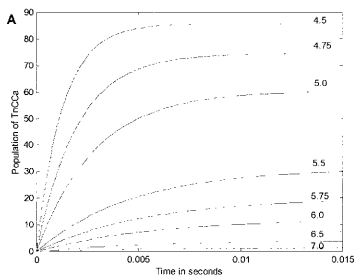
Fig. 7A. Time Course of Formation of TnCCa in the NTG Model
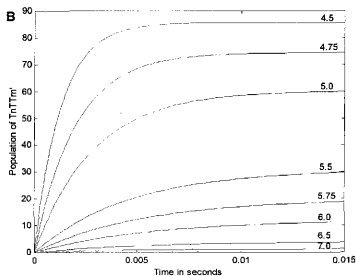
Fig. 7B. Time Course of Formation of TnTTm' in the NTG Model

Fig. 7C shows increase in population of Tm_{on1} for same Ca^{2+} levels. Rate of increase is sluggish for lower Ca^{2+} levels, but increases until it is very high for pCa = 4.5. The steady-state population is very low even at high Ca^{2+} levels, indicating that most of the thin filament units are trapped in 'on' state, Tm_{on2}, as seen from Fig. 7D. At pCa 7.0, understandably, population of Tm_{on2} is very low, since there are not enough strong CBs to trap them in 'on' state. As Ca^{2+} level increases, population of Tm_{on2} increases appreciably until almost 95% of thin filament population is in 'fully on' state. Fig. 7E shows time curves for the increase in population of weak bound CBs for different Ca^{2+} levels. The plot shows that at low Ca^{2+} levels most of the CBs are in weak bound state since rate of isomerization to strong bound state is low. As Ca^{2+} level rises, most of the CBs quickly isomerize to strong bound state, decreasing population of CBs in weak bound state. Also the plot shows that at low Ca^{2+} levels, rate of formation is low and increases with Ca^{2+} level. In contrast, steady state population first increases with increase in Ca^{2+} but after pCa 6.5, steady state population progressively decreases while rate of formation progressively increases.
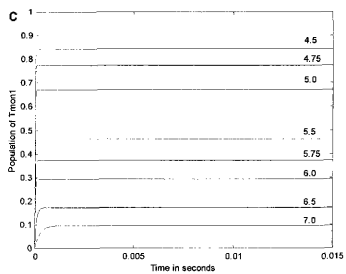
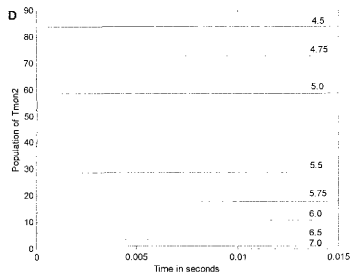**Fig. 7C. Time Course of Formation of Tm$_{on1}$ in the NTG Model**

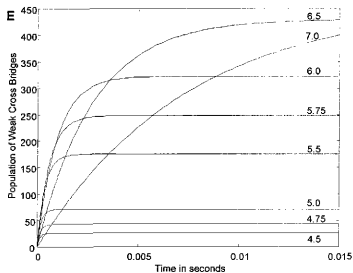**Fig. 7D. Time Course of Formation of Tm$_{on2}$ in the NTG Model**

Fig. 7E. Time Course of Formation of Weak CBs in the NTG Model

This suggests that CBs bind more easily to thin filament at higher Ca^{2+} levels since the filament is turned 'on'.

Fig. 7F shows time curves for increase in population of strong bound CBs prior to Pi release. Steady state population increases with increasing Ca^{2+} concentration, as expected, since more number of thin filaments are turned 'on'. Steady state population is low at low Ca^{2+} (pCa 7.0, 6.5). The level increases fairly rapidly in the interval pCa 6.0 to 5.0 after which steady state level begins to saturate indicating maximum CB turnover.

Fig. 7G shows similar set of time curves for force producing CBs at different Ca^{2+} levels. Steady state force increases with increasing Ca^{2+} concentration and begins to saturate at pCa 5.0. Fig. 7H shows formation of rigor CBs. Figs. 7I and 7J are plots of force and % maximal force respectively versus Ca^{2+} concentration. Force is plotted as steady state population of force CBs at each Ca^{2+} concentration, assuming that force produced is linearly proportional to population of force CBs. Since population is dimensionless, this allows representation of force as a dimensionless quantity. Experimental values of force are in the range of 0-50 mN/mm^2.

However, for our purpose, it is sufficient to assume unit dimensionless force quantity represented by the steady state value of force CBs.
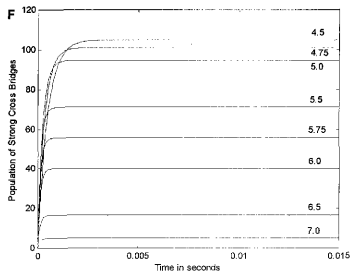

Fig. 7F. Time Course of Formation of Strong CBs in the NTG Model

From Fig. 7J, 50% of maximal force is achieved at a Ca^{2-} concentration of around pCa 5.8. This closely agrees with the experimental value of pCa 5.65 for NTG myofilaments.

For the TG model, key parameters that, when changed, would lead to increased Ca^{2+} sensitivity and decreased maximum force and ATPase activity, as compared to NTG model, were identified. Effects of changing any one of the key parameters are presented in the following pages. Parameters for which the model was tested are – (1) Rate of thin filament switching (k_5/k_6), (2) Rate of ismerization (k_{11}/k_{12}), (3) Rate of rigor CB formation (k_{15}) and (4) Rate of attachment (k_9).
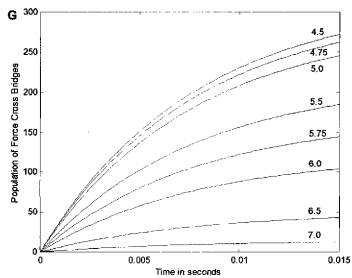
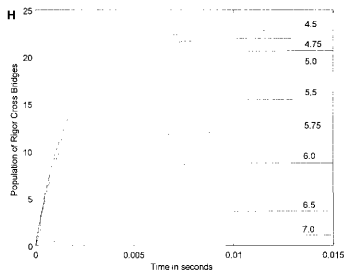**Fig. 7G. Time Course of Formation of Force CBs in the NTG Model**

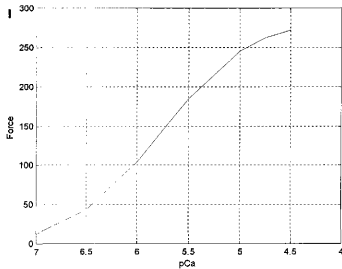**Fig. 7H. Time Course of Formation of Rigor CBs in the NTG Model**

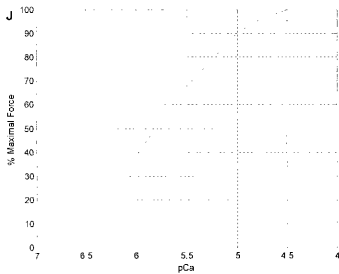**Fig. 7I. Plot of Force Versus Calcium Concentration in the NTG Model**

Fig. 7J. Plot of % Maximal Force Versus Calcium Concentration in the NTG Model

3.2. Calcium Sensitivity in the Transgenic Model

3.2.1. Case I: Increase in Rate of Thin Filament Switching

Effect of reduced affinity of β-Tm to TnT and actin was studied by increasing rate of thin filament switching. This was achieved by simultaneously increasing a_5 (the rate constant in the relation for k_5) and decreasing a_6 (the rate constant in the relation for k_6). Value of a_5 was increased 100 fold above its original value of 12.2 s^{-1} while value of a_6 was similarly reduced from 487.8 s^{-1} to 4.878 s^{-1}.

For this and all intermediate values, output of the model showed changes only in rate of increase in population of Tm_{on1} and its steady state levels. Fig. 8 shows effects of this change. Other than this change, every other output of the model remained unaffected.
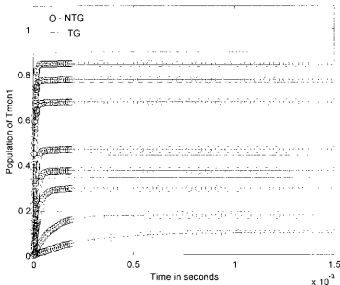

Fig. 8. Comparison of Rates of Formation of Tm_{on1} Between NTG and TG Models in Case I

(a_5 increased to 1220 s^{-1} and a_6 decreased to 4.878 s^{-1})

3.2.2. Case II: Increase in Rate of Isomerization from Weak Bound to Strong Bound Cross Bridges

The hypothesis tested here is that since Tm binds more weakly to actin in the TG case, ability of strong bound CBs in activating the thin filament is increased. This is interpreted as an increase in rate of isomerization of CBs from weak bound to strong `bound state. Rate constant a_{11} was increased from its original value of 90 s^{-1} by 10% to a value of 100 s^{-1} while rate constant a_{12} was decreased from its original value of 85 s^{-1} by 10% onwards. Rate of isomerization was increased in this manner to give different values. Figs. 9A to 9F show the typical output of an increase in this rate. For this output, forward rate a_{11} was increased to 100 s^{-1} (10% increase) and reverse rate a_{12} was decreased to 64 s^{-1} (25% decrease).
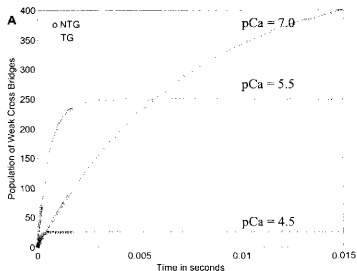

Fig. 9A. Comparison of Population of Weak CBs Between NTG and TG Models in Case II

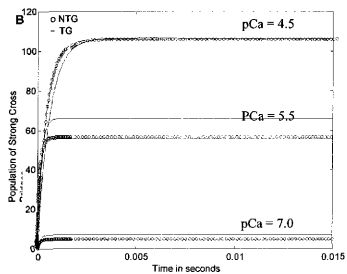**(a_{11} = 100 s^{-1}, a_{12} = 64 s^{-1})**

Fig. 9B. Comparison of Population of Strong CBs Between NTG and TG Models in Case II

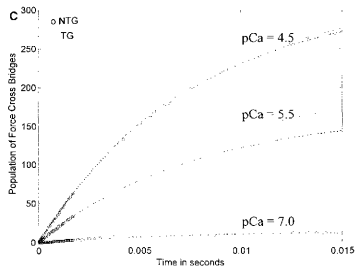$(a_{11} = 100 \text{ s}^{-1}, a_{12} = 64 \text{ s}^{-1})$

Fig. 9C. Comparison of Population of Force CBs Between NTG and TG Models in Case II

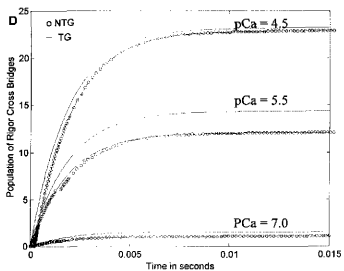$(a_{11} = 100 \text{ s}^{-1}, a_{12} = 64 \text{ s}^{-1})$

Fig. 9D. Comparison of Population of Rigor CBs Between NTG and TG Models in Case II

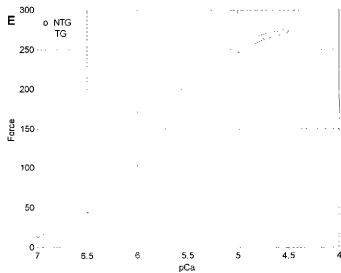$(a_{11} = 100 \text{ s}^{-1}, a_{12} = 64 \text{ s}^{-1})$

Fig. 9E. Comparison of Force Between NTG and TG Models in Case II

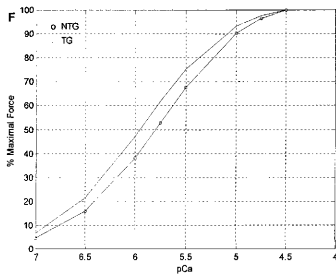$(a_{11} = 100 \text{ s}^{-1}, a_{12} = 64 \text{ s}^{-1})$

Fig. 9F. Comparison of % Maximal Force Between NTG and TG Models in

Case II ($a_{11} = 100$ s^{-1}, $a_{12} = 64$ s^{-1})

As seen from Fig. 9F, increasing rate of isomerization increased Ca^{2+} sensitivity of output. Other effects of increasing rate of isomerization include an increase in population of strong CBs (Fig. 9B) at low pCa, with saturation level reached earlier than in the NTG model, and with corresponding decrease in population of weak CBs (Fig. 9A). However, force also increased at every pCa (Fig. 9C and 9E). Rigor CB population increased significantly at low pCa but returned to control values at high pCa.

Further increases in rate of isomerization, caused by either increasing a_{11} or decreasing a_{12}, shifted the pCa - % maximal force curve further to the left with respect to NTG, indicating increasing Ca^{2+} sensitivity.

3.3. Decreased Force Production in the Transgenic Model

3.3.1. Case III: Increase in Rate of Rigor Cross Bridge Formation

In order to test the hypothesis that increase in rate of rigor CB formation leads to decrease in force production, rate constant k_{15} was increased from its original value of 45 s^{-1} in the NTG model to 90 s^{-1} (2-fold increase). Figs. 10A to 10F show the result of such a change in the TG model in comparison with the NTG model. All intermediate values produced similar effects.
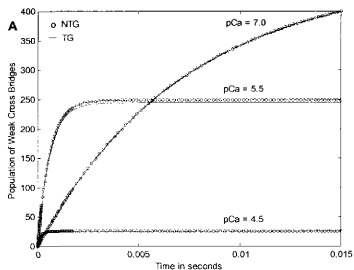

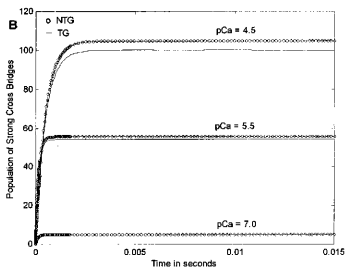Fig. 10A. Comparison of Population of Weak CBs Between NTG and TG Models in Case III (k_{15} = 90 s^{-1})

Fig. 10B. Comparison of Population of Strong CBs Between NTG and TG Models in Case III ($k_{15} = 90$ s^{-1})
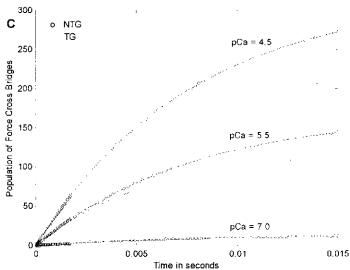

Fig. 10C. Comparison of Population of Force CBs Between NTG and TG Models in Case III ($k_{15} = 90$ s^{-1})
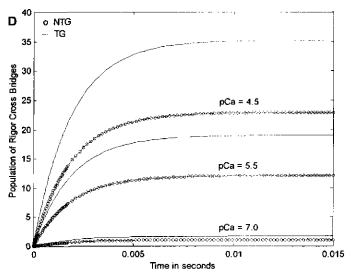
Fig. 10D. Comparison of Population of Rigor CBs Between NTG and TG Models in Case

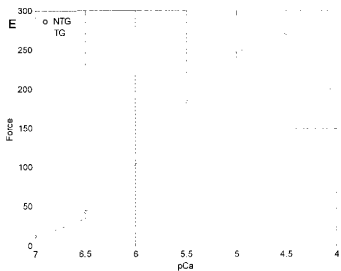**III ($k_{15} = 90$ s^{-1})**

Fig. 10E. Comparison of Force Between NTG and TG Models in Case III
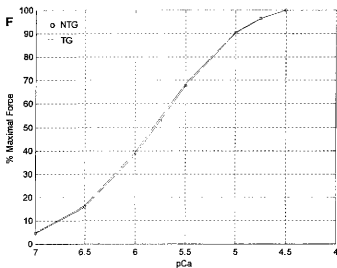
($k_{15} = 90$ s^{-1})

Fig. 10F. Comparison of % Maximal Force Between NTG and TG Models in

Case III ($k_{15} = 90$ s^{-1})

Effect of increasing rate of rigor CB formation is to decrease force at all Ca^{2+} levels. Figs. 10A, 10B and 10C show respectively, populations at Ca^{2+} levels pCa 7, 5.5 and 4.5. There is a decrease in force even if there is no decrease in ATPase activity. Though there is no change in rate of attachment, a faster rate of transition of CBs into rigor-state, with no change in rates of any of the intermediate steps, results in a slight decrease in population of strong CBs at high Ca^{2+} levels. With fewer numbers of CBs isomerizing to strong bound state and a faster rate of transition into rigor states, population of force CBs also decreases. The slight left shift seen in the % maximal force - pCa curve with respect to NTG is entirely due to decreased force at all Ca^{2+} levels and does not indicate increased Ca^{2+} sensitivity of the CB cycling process.

3.3.2. Case IV: Decrease in Rate of Attachment

Decreasing rate of attachment (k_9) decreased population of all the states following it (See Figs. 11A to 11F). Value of k_9 was decreased from its original value of 1.5e6 $M^{-1}s^{-1}$ to 0.75e6 $M^{-1}s^{-1}$ (50% decrease). This and all other intermediate values showed the same effect.

Fig. 11A. Comparison of Population of Weak CBs Between NTG and TG Models in Case IV ($k_9 = 0.75e6\ M^{-1}s^{-1}$)

Fig. 11B. Comparison of Population of Strong CBs Between NTG and TG Models in Case IV ($k_9 = 0.75e6\ M^{-1}s^{-1}$)

Fig. 11C. Comparison of Population of Force CBs Between NTG and TG Models in Case IV ($k_9 = 0.75e6$ M^{-1}s^{-1})

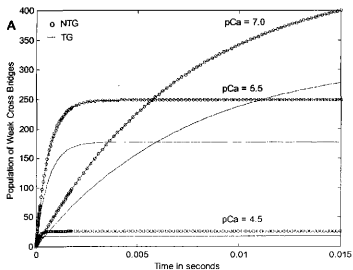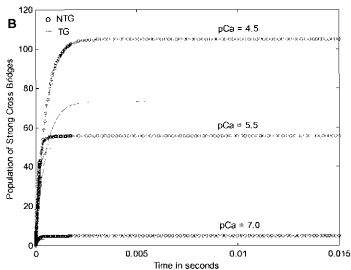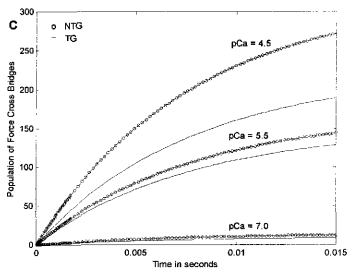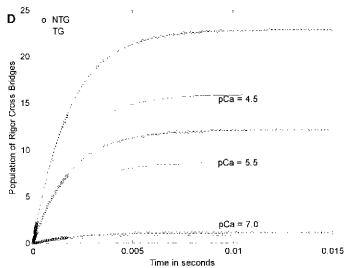**Fig. 11D. Comparison of Population of Rigor CBs Between NTG and TG Models in Case IV ($k_9 = 0.75e6$ M^{-1}s^{-1})**
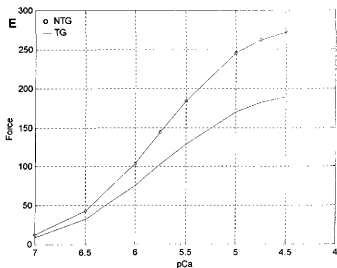
Fig. 11E. Comparison of Force Between NTG and TG Models in
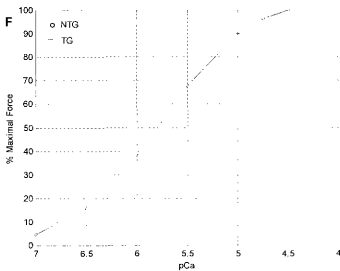Case IV ($k_9 = 0.75e6$ M^{-1}s^{-1})

Fig. 11F. Comparison of % Maximal Force Between NTG and TG Models in
Case IV ($k_9 = 0.75e6$ M^{-1}s^{-1})

Decrease in the population of strong CBs at high Ca^{2+} levels indicates reduced ATPase activity.

The above evaluations led to the conclusion that in order to achieve the experimental result of increased Ca^{2+} sensitivity and decreased force production, one of these options is true -

1. Increase in rate of isomerization coupled with increase in rate of rigor CB formation
2. Increase in rate of isomerization coupled with decrease in rate of attachment

3.4. Case V: Increase in Rate of Isomerization and Rate of Rigor Cross Bridge Formation

Increase in rate of isomerization is achieved by increasing a_{11} and decreasing a_{12} and increase in rate of rigor CB formation is achieved by increasing k_{15}. Figs. 12A to 12F show a typical output obtained for the following values: $a_{11} = 100$ s^{-1}, $a_{12} = 64$ s^{-1}, $k_{15} = 90$ s^{-1}.

Output obtained with this combination of parameter changes satisfies most of the experimental observations, except for decrease in maximum ATPase activity. Fig. 12A shows that decrease in population of weak CBs is greater as compared to the NTG model. This is due to increase in rate of isomerization. Correspondingly, there is an increase in population of strong CBs at low Ca^{2+} concentrations. At high Ca^{2+} levels, the population saturates, with steady state level being slightly less than that of the NTG model. However, this decrease is negligible and hence ATPase activity is almost same as that of the NTG model. Force developed is higher at low pCa but decreases below control values for pCa values greater than 6. At the same time, population of rigor CBs increases significantly for all pCa values. By virtue of an increase in rate of isomerization, the TG model also exhibits Ca^{2+} sensitivity as seen from Fig. 12F.

Fig. 12A. Comparison of Population of Weak CBs Between NTG and TG Models in Case V

$$(a_{11} = 100 \text{ s}^{-1}, a_{12} = 64 \text{ s}^{-1}, k_{15} = 90 \text{ s}^{-1})$$
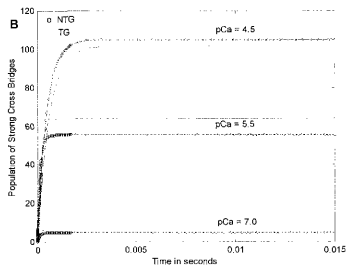
Fig. 12B. Comparison of Population of Strong CBs Between NTG and TG Models in Case

$$V \ (a_{11} = 100 \text{ s}^{-1}, a_{12} = 64 \text{ s}^{-1}, k_{15} = 90 \text{ s}^{-1})$$
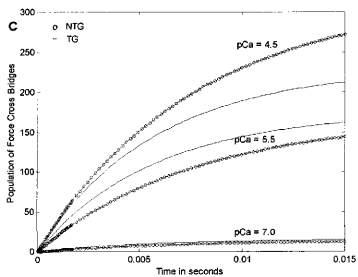
Fig. 12C. Comparison of Population of Force CBs Between NTG and TG Models in Case V

$$(a_{11} = 100 \text{ s}^{-1}, a_{12} = 64 \text{ s}^{-1}, k_{15} = 90 \text{ s}^{-1})$$

Fig. 12D. Comparison of Population of Rigor CBs Between NTG and TG Models in Case V

$$(a_{11} = 100 \text{ s}^{-1}, a_{12} = 64 \text{ s}^{-1}, k_{15} = 90 \text{ s}^{-1})$$

Fig. 12E. Comparison of Force Between NTG and TG Models in Case V

$(a_{11} = 100 \text{ s}^{-1}, a_{12} = 64 \text{ s}^{-1}, k_{15} = 90 \text{ s}^{-1})$
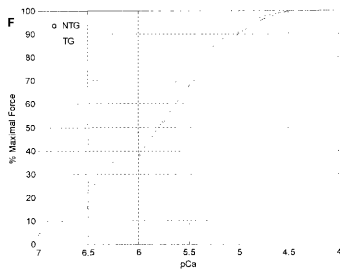
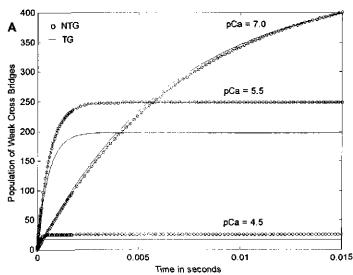**Fig. 12F. Comparison of % Maximal Force Between NTG and TG Models in Case V** $(a_{11} = 100 \text{ s}^{-1}, a_{12} = 64 \text{ s}^{-1}, k_{15} = 90 \text{ s}^{-1})$
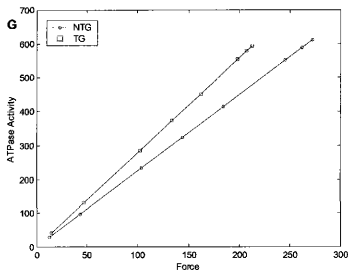
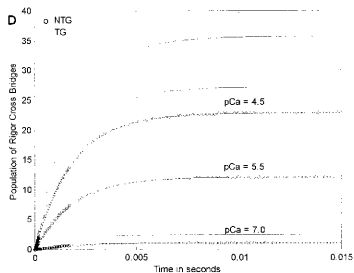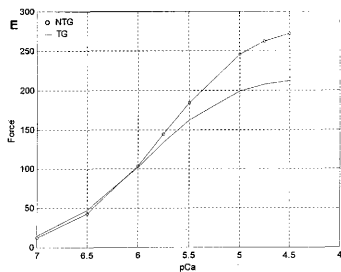**Fig. 12G. Plot of ATPase Activity Versus Force in Case V**

The Ca^{2-} concentration at which the TG model achieves 50% of its maximal force is about pCa 5.9. Experimental value obtained for pCa_{50} in the TG model is around 5.8. Hence output obtained by the model is in quite close agreement with experimental data. Moreover, this combination of parameters satisfies experimental observations of increased Ca^{2+} sensitivity and decreased force production. However, there is no corresponding decrease in maximum ATPase activity, since population of strong CBs at maximum Ca^{2+} levels does not differ from control. Experimental observations indicate that the slope of the relationship is same for both NTG as well as TG systems, whereas Fig. 12G shows difference in slopes between the two systems. Moreover, there is an increase in population of rigor CBs, indicating decrease in CB turnover, whereas experimental evidence suggested otherwise.

3.5. Case VI: Increase in Rate of Isomerization and Decrease in Rate of Attachment

Increase in rate of isomerization is achieved as mentioned previously. Rate of attachment is decreased by 10% in successive runs. A typical output is shown in Figs. 13A to 13F for an attachment rate value of 0.975e6 $M^{-1}s^{-1}$ (35% decrease) with $a_{11} = 100$ s^{-1} and $a_{12} = 64$ s^{-1}. As before, Ca^{2+} sensitivity of output force is increased due to increase in rate of isomerization (Fig. 13F). Force versus pCa curve (Fig. 13E) also shows increased force at low Ca^{2+} and decreased force at high Ca^{2+} levels.
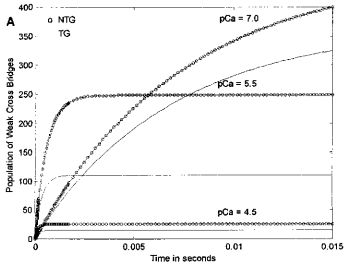
Fig. 13A. Comparison of Population of Weak CBs Between NTG and TG Models in Case

VI ($a_{11} = 100$ s^{-1}, $a_{12} = 64$ s^{-1}, $k_9 = 0.975$e6 M^{-1}s^{-1})
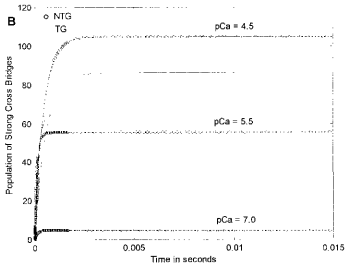
Fig. 13B. Comparison of Population of Strong CBs Between NTG and TG Models in Case

VI ($a_{11} = 100$ s^{-1}, $a_{12} = 64$ s^{-1}, $k_9 = 0.975$e6 M^{-1}s^{-1})
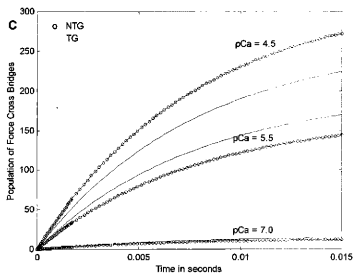
Fig. 13C. Comparison of Population of Force CBs Between NTG and TG Models in Case VI (a_{11} = 100 s^{-1}, a_{12} = 64 s^{-1}, k_9 = 0.975e6 M^{-1}s^{-1})
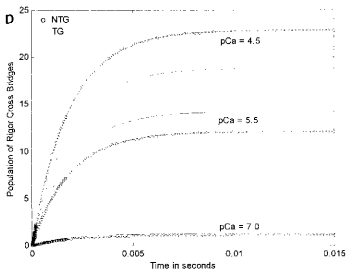
Fig. 13D. Comparison of Population of Rigor CBs Between NTG and TG Models in Case VI (a_{11} = 100 s^{-1}, a_{12} = 64 s^{-1}, k_9 = 0.975e6 M^{-1}s^{-1})
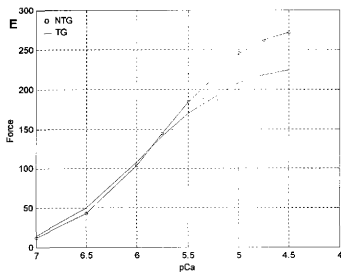
Fig. 13E. Comparison of Force Between NTG and TG Models in Case VI

$(a_{11} = 100 \ s^{-1}, \ a_{12} = 64 \ s^{-1}, \ k_9 = 0.975e6 \ M^{-1}s^{-1})$
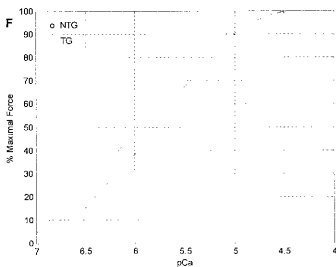
Fig. 13F. Comparison of % Maximal Force Between NTG and TG Models in

**Case VI $(a_{11} = 100 \ s^{-1}, \ a_{12} = 64 \ s^{-1}, \ k_9 = 0.975e6 \ M^{-1}s^{-1})$**
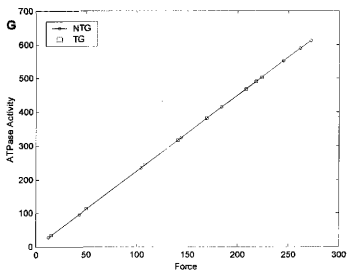
Fig. 13G. Plot of ATPase Activity Versus Force in Case VI

Decrease in population of strong CBs (Fig. 13B) at high Ca^{2+} concentrations indicates decrease in ATPase activity as compared to control. Further, plot of ATPase activity versus force (Fig. 13G) indicates linear correlation between ATPase activity and force with same slope, similar to experimental observations. Correspondingly there is a decrease in population of rigor CBs also at high Ca^{2+} levels. This combination of parameter changes accounts for every experimental observation. Further decrease in rate of attachment decreases force as well as decreases population of strong CBs and rigor CBs. A summary of the results obtained from the model is given in Table 2.

Table 2. *Summary of Results*

Parameter	Value		Force	Calcium Sensitivity	ATPase
	NTG	TG			
CASE I	$k_{11}/k_{12} = 90/85$	$k_{11}/k_{12} = 100/64$	Increase for all pCa	Increase	
CASE II	$k_5/k_6 =$ 12.2 /487.8	$k_5/k_6 =$ 1220/4.878	No Change	No Change	
CASE III	$k_{15} = 45$	$k_{15} = 90$	Decrease for all pCa	Negligible Increase	
CASE IV	$k_9 = 1.5e6$	$k_9 = 0.75e6$	Decrease for all pCa	No Change	
CASE V	$k_{11}/k_{12} = 90/85$, $k_{15} = 45$	$k_{11}/k_{12} = 100/64$, $k_{15} = 90$	Crossover at pCa = 6	Increase	Increased slope
CASE VI	$k_{11}/k_{12} = 90/85$, $k_9 = 1.5e6$	$k_{11}/k_{12} = 100/64$, $k_9 = 0.975e6$	Crossover at pCa = 5.9	Increase	Same slope

4. DISCUSSION AND CONCLUSIONS

The molecular model described in this research defines mechanisms that modulate thin filament protein interactions during myofilament contraction. Though many Ca^{2+}-regulated CB activation models have been proposed, this is the first time that individual thin filament proteins have been incorporated as different variables in the myofilament activation process. This facilitates testing effects of changes in any of the proteins, similar to those occurring in heart failure, on myofilament activation. In this research, effect of Tm alteration is studied.

Similar models can be formulated to test effects of perturbations in other thin filament proteins in isolation such as TnI and TnT, both of which are known to play significant roles in the activation process. Moreover, it allows insight into probable differences in mechanisms caused due to the change. Further validation with experimental results to support theoretical predictions would help in understanding contractile mechanisms during normal and diseased states.

This model includes a cooperativity feature in the activation of thin filament by making it dependent on the presence of at least one strong CB. Moreover, effect of Ca^{2+} regulation on CB kinetics is evident in the isomerization of a CB from a weak state to a strong state.

The activation process in the model is sequential in that rate of every step in the process is dependent on the output of the previous step. The stoichiometric ratio of thin filament composition is 1:1:7 for Tn:Tm:Actin. This ratio has been maintained by formulating rate relationships in such a manner that the forward reaction proceeds at a fast rate in the presence of the previous output, but when the two populations become equal, rate falls to zero and the reaction stops. This not only maintains an upper limit on the rate but also ensures that number of Tm molecules that are turned on does not exceed number of TnC that binds to Ca^{2+}. With these features, the model has provided similar value closure to experimental results on Ca^{2+} sensitivity and force production, implying that the model represents myofilament activation as it happens in the system.

The model was tested for the TG myofilament system by varying certain rate values in order to obtain the differences in Ca^{2+} sensitivity and force production observed in β-Tm TG mouse heart in comparison with NTG heart. Results obtained due to such changes indicate that switching Tm isoform population in the myofilament affects kinetics of the CB cycling process in two ways. First, it increases Ca^{2+} sensitivity of the process by promoting formation of strong

CBs at lower Ca^{2+} concentrations. At the same time, it tends to decrease steady state tension at high Ca^{2+} levels. The results obtained from the model prove that increase in Ca^{2+} sensitivity occurs due to increase in rate of isomerization of a weak bound CB to a strong bound state. Second, decrease in maximum force occurs due to either increase in rate of rigor CB formation or slight decrease in rate of attachment (about 35%).

It has been determined experimentally that β-Tm binds more weakly to TnT than α-Tm (26). There is significant amino acid similarity between striated muscle α- and β-Tm isoforms (86%). β-Tm exhibits 39 amino acid differences from α-Tm, 25 of which occur in the carboxyl domain, the region important for head-to-tail and TnT interaction. Important charge modifications in β-Tm are exchange of serine and histidine amino acids at positions 229 and 276 in α-Tm with glutamic acid and asparagene respectively (Ser229Glu and His276Ans), imparting to β-Tm a more negative charge relative to α-Tm (23). This difference in charge may partially account for weaker binding of β-Tm in fast skeletal muscle TnT than α-Tm. Moreover, Tm mutants causing FHC have been found to have 2 to 3-fold reduced affinity to the actin filament (9). Decreased affinity is seen regardless of ionic conditions and presence of Tn with or without Ca^{2+}. Reduced affinity of Tm to TnT at its ends and also to actin could lead to increased flexibility of the Tm molecule resulting in an enhanced rate of isomerization.

Rate of isomerization is also related to rate of force development. It has been determined experimentally that this rate is highly sensitive to Ca^{2+} in fast skeletal muscle (10) whereas cardiac muscle is much less sensitive to Ca^{2+} (46). Since αβ-heterodimer formation of Tm is a chief skeletal muscle feature, increased Ca^{2-} sensitivity may reflect activation and CB kinetics similar to skeletal muscle.

Best results matching experimental observations were obtained by decreasing rate of attachment of CBs by 35% along with increasing rate of isomerization. Decrease in rate of attachment decreases overall strong bound CB population, even though there is a corresponding increase in rate of isomerization. This suggests that rate of attachment of myosin heads to actin may be the rate-limiting step in the CB cycling process, when there is an exchange in Tm isoform. This is in keeping with the model proposed by Geeves and Lehrer (8), on which the proposed model is based.

Rate of attachment of myosin heads to actin can potentially be modulated by phosphorylation of myosin binding protein C (My-BPC), a protein that binds to both thick and thin filaments in the sarcomere (43,44). When phosphorylated, it is found that flexibility of CBs

is increased. Thus CB flexibility is an important parameter in setting rate of CB attachment. Whether β-Tm plays a role in determining flexibility of myosin heads is a theory to be explored.

Phosphorylation of TnI plays a major role in regulating relaxation rates of cardiac muscle and also affects Ca^{2+} sensitivity of myofilaments (38,39). However, when TnI was phosphorylated in β-Tm containing myofilaments, the effect was minimized or lost (24), suggesting that β-Tm may have weaker cooperative interactions with TnI, actin, and TnT. In addition, recent studies from Muthuchamy's group have suggested a functional interaction between TnI and My-BPC phosphorylation. Since in TG-β-Tm mouse, the effect of TnI phosphorylation is lost, we hypothesize that the My-BPC effect would have also been affected subsequently affecting rate of attachment. Experiments with My-BPC phosphorylated TG β-Tm myofilaments can provide answers to this hypothesis.

A combination of increase in rate of isomerization and increase in rate of rigor CB formation led to increase in Ca^{2+} sensitivity and decreased force at high Ca^{2+} levels. However, it is accompanied by increase in rigor CB population and unchanged maximum ATPase activity. Increase in rigor CB population suggests a corresponding increase in ADP release, contrary to experimental observations, where ATPase activity was linearly correlated to force with same slopes for both TG and NTG systems (47).

4.1. Limitations of the Model

The model does not account for effects of TnI and TnT as part of thin filament activation processes. Both TnI and TnT play important roles in thin filament activation and influence binding of myosin heads to actin in absence of Ca^{2+}. When TnI is phosphorylated, it is seen to decrease Ca^{2+} sensitivity of the fiber due to its reduced affinity to TnC in presence of Ca^{2+} (38,39). When functionally significant sites on TnT are phosphorylated, maximum ATPase activity is depressed without any change in the pCa-ATPase activity relation (38,39). Additionally, interactions between TnI and TnT as well as TnI and TnC are not accounted for in the model. Since myofilaments from TG β-Tm hearts, when subjected to TnI phosphorylation, did not produce any change in Ca^{2+} sensitivity, it is apparent that one of several outcomes of isoform switching was to nullify the effect of TnI phosphorylation. This could be an important factor in the modulation of CB kinetics, which has not been considered in the model.

The model does not account for length changes during contraction. Maximum speed of shortening, as well as force produced, is directly related to the resting length of a fiber. Length

dependence of force produced by a myofilament follows the Frank-Starling mechanism, which states that maximum force is produced at an optimal length. Any change in length below or beyond the optimum value leads to a decrease in force produced.

The model does not account for passive elements contributing to steady state tension. Force released by the myosin head after binding to actin is the active force that produces a strain in the CB. This strain is communicated to elastic components in the contractile unit, 'connectin' and 'titin'. Actual steady state tension is a cumulative effect of active chemical force, mechanical and passive elastic force.

The model assumes constant ATP concentration. Further, it considers only those steps in the CB cycle that are essential for the purpose of this research. However, it is known that the actin-myosin ATPase cycle consists of many conformational changes occurring in the myosin head, each contributing a different property or effect in the process. Few rates in this process are Ca^{2+} dependent while others are ATP concentration dependent (6,11,19,31,37). A complete model would include all the steps in the CB cycling process as well as all the proteins in the thick and thin filaments. However, all the states in the CB cycling are not yet identified and characterized.

4.2. Conclusion

In conclusion, this research defines probable mechanisms occurring as a result of Tm isoform switching in myofilaments via a model that incorporates details of thin filament activation, a crucial regulating step in the CB cycling process. Data from this study determines that effects of Tm isoform switching is to – (1) increase rate of isomerization leading to increase in Ca^{2+} sensitivity and (2) decrease rate of attachment of myosin heads to the actin filament leading to a decrease in force production. These changes in CB kinetics produce the output as observed through experiments. A role for β-Tm in influencing the effect of TnI phosphorylation as well as in affecting CB flexibility has been suggested. This model is a new approach in attempting to study separately the properties of various protein chains involved in myofilament activation and contraction. In this research, the effect of Tm isoform switching is studied and its important role in the process of thin filament activation is established.

REFERENCES

1. **Al-Khayat, H.A., Yagi, N., Squire, J.M.** Structural changes in actin-tropomyosin during muscle regulation: computer modelling of low angle X-ray diffraction data. *J. Mol. Biol.* 252: 611-632, 1995.

2. **Bottinelli, R., Coviello, D.A., Redwood, C.S., Pellegrino, M.A., Maron, B.J., Spirito, P. Watkins, H., Reggiani, C.** A mutant tropomyosin that causes hypertrophic cardiomyopathy is expressed in vivo and associated with an increased calcium sensitivity. *Circ. Res.* 82: 106-115, 1998.

3. **Campbell, K.** Rate constant of muscle force redevelopment reflects cooperative activation as well as cross-bridge kinetics. *Biophys. J.* 72: 254-262, 1997.

4. **Capellos, C., Bielski, B.H.J.** *Kinetic Systems: Mathematical Description of Chemical Kinetics in Solution.* New York, NY: John Wiley & Sons, Inc., 1972.

5. **Coates, J.H., Criddle, A.H., Geeves, M.A.** Pressure-relaxation studies of pyrene-labelled actin and myosin subfragment 1 from rabbit skeletal muscle. *Biochem. J.* 232: 351-356, 1985.

6. **Dantzig, J.A., Hibberd, M.G., Trentham, D.R., Goldman, Y.E.** Cross-bridge kinetics in the presence of MgADP investigated by photolysis of caged ATP in rabbit psoas muscle fibers. *J of Phys.* 432: 639-680, 1991.

7. **Dong, W., Rosenfeld, S.S., Wang, C., Gordon, A.M., Cheung, H.C.** Kinetic studies of calcium binding to the regulatory site of troponin C from cardiac muscle. *J Biol. Chem.* 271: 688-694, 1996.

8. **Geeves, M.A., Lehrer, S.S.** Dynamics of the thin filament regulatory switch: the size of the cooperative unit. *Biophys. J.* 67: 273-282, 1994.

9. **Golitsina, N., An, Y., Greenfield, N.J., Thierfelder, L., Iizuka, K., Seidman, J.G., Seidman, C.E., Lehrer, S.S., Hitchcock-DeGregori, S.E.** Effects of two familial hypertrophic cardiomyopathy-causing mutations on α-tropomyosin structure and function. *Biochemistry.* 36: 4637-4642, 1997.

10. **Hancock, W.O., Huntsman, L.L., Gordon, A.M.** Models of calcium activation account for differences between skeletal and cardiac force redevelopment kinetics. *J Mus. Res. Cell Mot.* 18: 671-681, 1997.

11. **Hibberd, M.G., Dantzig, J.A.** Phosphate release and force generation in skeletal muscle fibers. *Science.* 228: 1317-1319, 1985.

12. **Huxley, H.E.** The mechanism of muscular contraction. *Sci. Am.* 213: 18-27, 1965.

13. **Ishii, Y., Lehrer, S.S.** Excimer fluorescence of pyrenyliodoacetamide-labeled tropomyosin: a probe of the state of tropomyosin in reconstituted muscle thin filaments. *Biochemistry.* 29: 1160-1166, 1990.

14. **Ishijima, A., Kojima, H., Funatsu, T., Tokunaga, M., Higuchi, H., Tanaka, H., Yanagida, T.** Simultaneous observation of individual ATPase and mechanical events by a single myosin molecule during interaction with actin. *Cell.* 92: 161-171, 1998.

15. **Lehrer, S.S.** The regulatory switch of the muscle thin filament: Ca^{2+} or myosin heads? *J Mus. Res. Cell Mot.* 15: 232-236, 1994.

16. **Lorenz, M., Poole, K.J.V., Popp, D., Rosenbaum, G., Holmes, K.C.** An atomic model of the unregulated thin filament obtained by X-ray fiber diffraction on oriented actin-tropomyosin gels. *J. Mol. Biol.* 246: 108-119, 1995.

17. **McKillop, D.F.A., Geeves, M.A.** Regulation of the interaction between actin and myosin subfragment 1: evidence for three states of the thin filament. *Biophys. J.* 65: 693-701, 1993.

18. **Miki, M., Iio, T.** Kinetics of structural changes of reconstituted skeletal muscle thin filaments observed by fluorescence resonance energy transfer. *J Biol. Chem.* 268: 7101-7106, 1993.

19. **Millar, N.C., Homsher, E.** The effect of phosphate and calcium on force generation in glycerinated rabbit skeletal muscle fibers. *J Biol. Chem.* 265: 20234-20240, 1990.

20. **Moss. R.L.** Plasticity in the dynamics of myocardial contraction. Ca^{2+}, cross-bridge kinetics, or molecular cooperation. (Editorial) *Circ. Res.* 84: 862-865, 1999.

21. **Muthuchamy, M., Boivin, G.P., Grupp, I.L., Wieczorek, D.F.** β-tropomyosin overexpression induces severe cardiac abnormalities. *J. Mol. Cell. Cardiol.* 30: 1545-1557, 1998.

22. **Muthuchamy, M., Grupp, I.L., Grupp, G., O'Toole, B.A., Kier, A.B., Boivin, G.P., Neumann, J., Wieczorek, D.F.** Molecular and physiological effects of overexpressing striated muscle β-tropomyosin in the adult murine heart. *J. Biol. Chem.* 270: 30593-30603, 1995.

23. **Muthuchamy, M., Rethinasamy, P., Wieczorek, D.F.** Tropomyosin structure and function. *Trends Cardiovasc. Med.* 7: 124-128, 1997.

24. **Palmiter, K.A., Kitada, Y., Muthuchamy, M., Wieczorek, D.F., Solaro, R.J.** Exchange of β- for α-tropomyosin in hearts of transgenic mice induces changes in thin filament response to calcium, strong cross-bridge binding and protein phosphorylation. *J. Biol. Chem.* 271: 11611-11614, 1996.

25. **Palmiter, K.A., Solaro, R.J.** Molecular mechanisms regulating the myofilament response to calcium: Implications of mutations causal for familial hypertrophic cardiomyopathy. *Basic Res. Cardiol.* 92: Suppl. 1: 63-73, 1997.

26. **Pearlstone, J.R., Smillie, B.L.** Binding of troponin T to several types of tropomyosin: sensitivity to calcium in the presence of troponin C. *J. of Biol. Chem.* 257: 10587-10592, 1982.

27. **Rayment, I., Holden, H.M., Whittaker, M., Yohn, C.B., Lorenz, M., Holmes, K.C., Milligan, R.A.** Structure of the actin-myosin complex and its implications for muscle contraction. *Science.* 261: 58-65, 1993.

28. **Reddy, D.S.** Cellular and molecular biology of cardiac hypertrophy. *Current Science.* 72: 13-30, 1997.

29. **Regnier, M. Homsher, E.** The effect of ATP analogs on posthydrolytic and force development steps in skinned skeletal muscle fibers. *Biophys. J.* 74: 3059-3071, 1998.

30. **Regnier, M., Lee, D.M., Homsher, E.** ATP analogs and muscle contraction: Mechanics and kinetics of nucleoside triphosphate binding and hydrolysis. *Biophys. J.* 74: 3044-3058, 1998.

31. **Regnier, M., Martyn, D.A., Chase, P.B.** Calcium regulation of tension redevelopment kinetics with 2-deoxy-ATP or low [ATP] in rabbit skeletal muscle. *Biophys. J.* 74: 2005-2015, 1998.

32. **Regnier, M., Morris, C., Homsher, E.** Regulation of the cross bridge transition from a weakly to strongly bound state in skinned rabbit muscle fibers. *Am. J. Physiol.* 269: C1532-C1539, 1995.

33. **Rethinasamy, P., Muthuchamy, M., Hewett, T., Boivin, G., Wolska, B.M., Evans, C., Solaro, R.J., Wieczorek, D.F.** Molecular and physiological effects of α-tropomyosin ablation in the mouse. *Circ. Res.* 82: 116-123, 1998.

34. **Rice, J.J., Winslow, R.L., Hunter, W.C.** Comparison of putative cooperative mechanisms in cardiac muscle: length dependence and dynamic responses. *Am. J. Physiol.* 276 (*Heart Circ. Physiol.* 45): H1734-H1754, 1999.

35. **Rosenfeld, S.S., Taylor, E.W.** Kinetic studies of calcium binding to regulatory complexes from skeletal muscle. *J Biol. Chem.* 260: 252-261, 1985.

36. **Sherwood, L.** *Human Physiology: From Cells to Systems.* Belmont,CA: Wadsworth Publishing Company, 1997.

37. **Sleep, J.A., Hutton, R.L.** Exchange between inorganic phosphate and adenosine 5'-triphosphate in the medium by actomyosin subfragment 1. *Biochemistry.* 19: 1276-1283, 1980.

38. **Solaro, R.J., Rarick, H.M.** Troponin and tropomyosin: proteins that switch on and tune in the activity of cardiac myofilaments. *Circ. Res.* 83: 471-480, 1998.

39. **Solaro, R.J., Van Eyk, J.** Altered interactions among thin filament proteins modulate cardiac function. *J Mol. Cell. Cardiol.* 28: 217-230, 1996.

40. **Squire, J.M.** *Molecular Mechanisms in Muscular Contraction.* Boca Raton, FL: CRC Press, Inc., 1990.

41. **Swartz, D.R., Moss, R.L., Greaser, M.L.** Calcium alone does not fully activate the thin filament for S1 binding to rigor myofibrils. *Biophys. J.* 71: 1891-1904, 1996.

42. **Trybus, K.M., Taylor, E.W.** Kinetic studies of the cooperative binding of subfragment 1 to regulated actin. *Proc. Natl. Acad. Sci. USA.* 77: 7209-7213, 1980.

43. **Weisberg, A., Winegrad, S.** Relation between crossbridge structure and actomyosin ATPase activity in the rat heart. *Circ. Res.* 83: 60-72, 1998.

44. **Weisberg, A., Winegrad, S.** Alteration of myosin cross bridges by phosphorylation of myosin-binding protein C in cardiac muscle. *Proc. Natl. Acad. Sci. USA.* 93: 8999-9003, 1996.

45. **Williams, D.L., Jr., Greene. L.E., Eisenberg, E.** Cooperative turning on of the myosin subfragment 1 adenosinetriphosphatase activity by the troponin-tropomyosin-actin complex. *Biochemistry.* 27: 6987-6993, 1988.

46. **Wolff, M.R., McDonald, K.S., Moss, R.L.** Rate of tension development in cardiac muscle varies with level of activator calcium. *Circ. Res.* 76: 154-160, 1995.

47. **Wolska, B.M., Keller, R.S., Evans, C.C., Palmiter, K.A., Phillips, R.M., Muthuchamy, M., Oehlenschlager, J., Wieczorek, D.F., de Tombe, P.P., Solaro, R.J.** Correlation between myofilament response to calcium and altered dynamics of contraction and relaxation in transgenic cardiac cells that express β-Tm. *Circ. Res.* 84: 745-751, 1999.

48. **Yamaguchi, H., Takaki, M., Matsubara, H., Yasuhara, S., Suga, H.** Constancy and variability of contractile efficiency as a function of calcium and cross-bridge kinetics: simulation. *Am. J Physiol.* 270 (*Heart Circ. Physiol.* 39): H1501-H1508, 1996.

VITA

The youngest daughter of S. Krishnamoorthy and K. Annapoorni, Gayathri Krishnamoorthy hails from India. Born and brought up in the city of Mumbai (previously known as Bombay), she obtained her Bachelor of Engineering degree in Electronics from University of Mumbai in 1995. She joined Texas A&M University in fall 1997, and received her Master of Science degree in Biomedical Engineering in 1999. Her permanent address is 2, Gayatri, Chheda Nagar, Chembur, Mumbai - 400089, India.